

# Cooperative Output Regulation with Mixed Time- and Event-triggered Observers

Shimin Wang, Zhan Shu, Tongwen Chen

**Abstract**—Mixed time- and event-triggered cooperative output regulation for heterogeneous distributed systems is investigated in this paper. A distributed observer with time-triggered observations is proposed to estimate the state of the leader, and an auxiliary observer with event-triggered communication is designed to reduce the information exchange among followers. A necessary and sufficient condition for the existence of desirable time-triggered observers is established, and delicate relationships among sampling periods, topologies, and reference signals are revealed. An event-triggering mechanism based on local sampled data is proposed to regulate the communication among agents; and the convergence of the estimation errors under the mechanism holds for a class of positive and convergent triggering functions, which include the commonly used exponential function as a special case. The mixed time- and event-triggered system naturally excludes the existence of Zeno behavior as the system updates at discrete instants. When the triggering function is bounded by exponential functions, analytical characterization of the relationship among sampling, event triggering, and inter-event behaviour is established. Finally, several examples are provided to illustrate the effectiveness and merits of the theoretical results.

**Index Terms**—Pathological Sampling, Time-triggered observation, Event-triggered communication, Distributed control, Distributed systems.

## I. INTRODUCTION

Cooperative control of distributed systems has been extensively studied over decades, e.g., coupled oscillators [1, 2], consensus [3, 4], and formation control [5, 6]. An important class of cooperative control problems is cooperative output regulation, which includes leader-following consensus as a special case [7]. The problem of cooperative output regulation aims to design a distributed control law by using local information such that the regulated errors of agents converge to zero [8–10]. A comprehensive survey on cooperative output regulation for continuous- and discrete-time systems can be found in [11].

Communication constraints naturally exist in distributed systems, posing grand challenges to control analysis and design. Most existing cooperative control laws and protocols rely on continuous sensing and communication among agents, which is over-idealized and hard to implement. Therefore, more realistic designs based on intermittent signals are desired [12]. Time-triggered and event-triggered sampling schemes are two commonly used approaches in practice to generate

intermittent signals for estimation and control. With the time-triggered approach, continuous-time signals are often sampled periodically, resulting in periodic observations and control updates [13]. By contrast, with the event-triggered approaches, continuous-time signals are sampled according to prescribed or adaptive triggering conditions, leading to irregular observations and control updates [14–16], which may significantly reduce unnecessary consumption of resources. In this regard, cooperative control using the event-triggered approach has received a great deal of attention [17].

In particular, the event-triggered approach has been applied to the cooperative output regulation problem for both linear and nonlinear distributed systems [18–21]. For example, [19] proposed an event-triggered distributed observer to achieve cooperative output regulation by utilizing a self-triggering strategy, and the problem over switching networks was considered in [20]. Moreover, event-triggered robust cooperative output regulation for a class of linear minimum-phase distributed systems was considered in [18] by using an augmented system approach, and a more complex nonlinear version was studied in [21] by employing a distributed internal model design. However, to verify whether events should occur or not, the results aforementioned require continuous and real-time monitoring of the neighbours' states, which contradicts the original purpose of introducing event-based control as a means for reducing communication in distributed systems [22].

To reduce the dependence on real-time information of neighbour agents, recent efforts have focused on designing triggering mechanisms with localized information. In [23], an open-loop estimator was designed for each agent to estimate the neighbours' states and achieve leaderless synchronization. This estimator-based approach was further used to solve the event-triggered cooperative output regulation problem for linear distributed systems [24, 25]. In [26], a distributed observer involving multiple predictors and an edge-based triggering mechanism was proposed to remove the real-time inter-agent communication, and a similar approach was applied to cooperative output regulation with bounded inputs in [27].

All the results aforementioned are based on continuous-time signals of agents, and the triggering condition has to be monitored and verified continuously. However, most control algorithms and communication protocols are implemented with digital devices, resulting in clock-driven measurements and updates. Therefore, a great deal of effort has been devoted to developing various event-triggered strategies that are based on discrete-time signals of agents, among which the periodic event-triggered strategy has received much attention [22, 28, 29]. Very recently, the period event-triggered strategy

This work was supported by NSERC and an Alberta EDT Major Innovation Fund. Shimin Wang, Zhan Shu and Tongwen Chen are with Department of Electrical and Computer Engineering, University of Alberta, Edmonton, Alberta, T6G 1H9, Canada. Emails: shimin1@ualberta.ca, zshul@ualberta.ca, tchen@ualberta.ca

has been employed to the cooperative output regulation problem of linear distributed systems in [30]. With the periodic event-triggered strategy, the triggering condition is checked at discrete sampling instants, making it suitable for digital implementation. Also, it naturally excludes Zeno behavior, which is undesirable due to its impracticability [28]. Besides, the inter-event steps with the periodic event-triggered strategy are multiples of the sampling period, facilitating related protocol design. However, a significant design issue, periodic sampling, has rarely been treated in the existing literature. The sampling period in most cases is either selected as a sufficiently small number or restricted to some values on a fixed interval determined by a set of linear matrix inequalities or the spectral radius/norm of certain graph-induced matrix [22, 29–31]. Although some researchers have noticed the impact of the sampling period on consensus behaviour of second-order systems [32, 33], general results on the sampling period and its relationship with stability and performance of distributed systems are quite limited, especially for the cooperative output regulation problem, where extra reference or disturbance signals are involved. Apart from this, the interaction between periodic sampling and event triggering is poorly understood, and their impact on the inter-event dynamics remains unclear.

Motivated by the studies mentioned above, cooperative output regulation of heterogeneous distributed systems is investigated in this paper using *mixed time- and event-triggered observers* approach. The main contributions are summarized as follows:

- 1) Mixed time- and event-triggered observers are proposed to estimate the state of the leader with discontinuous monitoring and localized event triggering.
- 2) The interactions among sampling periods, topologies, reference signals, and related observability have been fully revealed, and all non-pathological / pathological sampling periods are given.
- 3) The convergence of the error dynamics holds for a class of convergent triggering functions, which include the commonly used exponential function as a special case.
- 4) The mixed time- and event-triggered architecture naturally excludes Zeno behavior. For a special class of triggering functions, which are bounded by exponential functions, inter-event behaviours have been analyzed, and their links with period sampling and event triggering have been revealed.

The rest of this paper is organized as follows: In Section II, the cooperative output regulation problem is formulated, and some standard assumptions are introduced. Section III is devoted to designing a pair of time-triggered and event-triggered observers and analyzing related stability. In Section IV, a distributed controller based on the designed mixed time- and event-triggered observers is proposed to achieve cooperative output regulation. Examples are provided in Section V to show the effectiveness and efficiency of the proposed approach, followed by conclusions given in Section VI.

**Notation:**  $\mathbb{R}$  and  $\mathbb{C}$  are the set of real numbers and the set of complex numbers, respectively.  $\mathbb{N}$  denotes all the natural num-

bers.  $\mathbb{Z}$  and  $\mathbb{Z}^+$  are the set of all integers and the set of positive integers, respectively.  $I_n$  denotes the  $n \times n$  identity matrix.  $\otimes$  represents the Kronecker product of matrices. For a collection of vectors  $b_i \in \mathbb{R}^{n_i \times p}$ ,  $\text{col}(b_1, \dots, b_m) \triangleq [b_1^T, \dots, b_m^T]^T$ . For a square matrix  $S \in \mathbb{R}^{n \times n}$ ,  $\lambda_q(S)$ ,  $q = 1, 2, \dots, n$ , represent its eigenvalues. For a complex number  $z \in \mathbb{C}$ ,  $\text{Re}(z)$  and  $\text{Im}(z)$  denote the real and imaginary parts of  $z$ , respectively;  $\text{Arg}(z) \in (-\pi, \pi]$  denotes the principal value of the argument of  $z$ ;  $|z|$  denotes the modulus of  $z$ ;  $z^*$  denotes the complex conjugate of  $z$ . For a matrix  $B \in \mathbb{R}^{m \times n}$ ,  $\|B\|$  stands for the 2-norm of  $B$ .

## II. PROBLEM FORMULATION AND ASSUMPTIONS

### A. Problem formulation

The distributed system considered in this paper involves a leader and  $N$  followers. They are connected through a network topology described by a digraph  $\mathcal{G} \triangleq (\mathcal{V}, \mathcal{E})$  with  $\mathcal{V} = \{0, \dots, N\}$  and  $\mathcal{E} \subseteq \mathcal{V}^2$ , where  $\mathcal{V}$  and  $\mathcal{E}$  represent the sets of vertices and edges, respectively. Throughout the paper, vertex 0 is associated with the leader and vertex  $i \in \mathcal{V}_F \triangleq \{1, 2, \dots, N\}$  is associated with each follower. For  $i \in \mathcal{V}$  and  $j \in \mathcal{V}_F$ , the ordered pair  $(i, j) \in \mathcal{E}$  represents that there is a directional communication link from agent  $i$  to agent  $j$ .  $\mathcal{N}_i \triangleq \{j | (j, i) \in \mathcal{E}\}$  denotes all the neighbors of agent  $i$ . The Laplacian of a digraph is represented by  $L = [l_{ij}] \in \mathbb{R}^{N+1}$ , where  $l_{ii} = -\sum_{j=1}^N l_{ij}$ ,  $l_{ij} = -1$  for  $i \neq j$  if  $(j, i) \in \mathcal{E}$ , and  $l_{ij} = 0$  for  $i \neq j$  otherwise.  $H \in \mathbb{R}^N$  denotes the leader-following matrix obtained by deleting the first row and column of  $L$  [8, 34]. More details on the graph theory can be found in [35].

The leader is described by the following autonomous differential equation

$$\dot{v}(t) = Sv(t), \quad (1)$$

where  $S \in \mathbb{R}^{n \times n}$  is the system matrix of the leader;  $v(t) \in \mathbb{R}^n$  is the state of the leader representing the reference signal to be tracked or the disturbance signal to be attenuated.

Each follower  $i$  is described by the following linear differential equation

$$\dot{x}_i(t) = A_i x_i(t) + B_i u_i(t) + P_i v(t), \quad (2a)$$

$$e_i(t) = C_i x_i(t) + D_i u_i(t) + F_i v(t), \quad (2b)$$

where  $x_i(t) \in \mathbb{R}^{n_i}$ ,  $u_i(t) \in \mathbb{R}^{m_i}$ , and  $e_i(t) \in \mathbb{R}^{l_i}$  are the state, the control input, and the regulated error of follower  $i$ , respectively;  $A_i \in \mathbb{R}^{n_i \times n_i}$ ,  $B_i \in \mathbb{R}^{n_i \times m_i}$ ,  $C_i \in \mathbb{R}^{l_i \times n_i}$ ,  $P_i \in \mathbb{R}^{n_i \times n}$ ,  $D_i \in \mathbb{R}^{l_i \times m_i}$ , and  $F_i \in \mathbb{R}^{l_i \times n}$  are known constant matrices for each  $i \in \mathcal{V}_F$ .

The distributed controller considered in this paper is of the form

$$\begin{aligned} u_i(t) &= \Xi_i(x_i(t), \eta_i(t)), \\ \dot{\eta}_i(t) &= \Theta_i(\eta_i(t), \eta_j(t), j \in \mathcal{N}_i), \end{aligned} \quad (3)$$

where  $\eta_i(t)$  is the estimation of  $v(t)$  generated by follower  $i$ ;  $\Theta_i$  and  $\Xi_i$  are mappings to be designed for each  $i \in \mathcal{V}_F$ .

Now, we formulate the problem to be tackled in this paper.

**Problem 1 (Cooperative Output Regulation):** Given the distributed system in (1) and (2), and a digraph  $\mathcal{G}$ , find a

distributed control law of the form (3) such that the closed-loop system is stable and, for  $i \in \mathcal{V}_F$  and any initial condition,

$$\lim_{t \rightarrow \infty} e_i(t) = 0.$$

### B. Assumptions

The following assumptions are essential to solve Problem 1.

*Assumption 1:*  $(A_i, B_i)$  is stabilizable, for  $i \in \mathcal{V}_F$ .

*Assumption 2:* The following linear matrix equations have solutions  $X_i$  and  $U_i$  for  $i \in \mathcal{V}_F$ :

$$X_i S = A_i X_i + B_i U_i + P_i, \quad (4a)$$

$$0 = C_i X_i + D_i U_i + F_i. \quad (4b)$$

*Assumption 3:*  $\mathcal{G}$  contains a spanning tree with vertex 0 as the root.

Assumptions 1 and 2 are standard for the regulation problem, while Assumption 3 is required for distributed observer design. Under Assumption 3, all eigenvalues of  $H$  have positive real parts, that is,  $\text{Re}(\lambda_i(H)) > 0$ , for  $i \in \mathcal{V}_F$ . According to the real parts of the eigenvalues of  $S$ , a partition of the set  $\mathcal{Q} = \{1, \dots, n\}$  is constructed as follows:

$$\mathcal{Q}_1 = \{q \mid \text{Re}(\lambda_q) > 0, q \in \mathcal{Q}\}, \quad (5a)$$

$$\mathcal{Q}_2 = \{q \mid \text{Re}(\lambda_q) < 0, q \in \mathcal{Q}\}, \quad (5b)$$

$$\mathcal{Q}_3 = \{q \mid \text{Re}(\lambda_q) = 0, \text{Im}(\lambda_q) \neq 0, q \in \mathcal{Q}\}, \quad (5c)$$

$$\mathcal{Q}_4 = \{q \mid \text{Re}(\lambda_q) = 0, \text{Im}(\lambda_q) = 0, q \in \mathcal{Q}\}. \quad (5d)$$

In the remaining of this paper,  $H$  and  $S$  in  $\lambda_i(H)$  and  $\lambda_q(S)$  are omitted for notational simplicity, as they can be deduced from the subscripts  $i$  and  $q$ . Also, suppose that the polar form of  $\lambda_i$  and  $\lambda_q$  can be written as

$$\lambda_i = |\lambda_i| e^{\theta_i j} \quad \text{and} \quad \lambda_q = |\lambda_q| e^{\theta_q j},$$

where  $\theta_i = \text{Arg}(\lambda_i)$  and  $\theta_q = \text{Arg}(\lambda_q)$  for  $q \in \mathcal{Q}$  and  $i \in \mathcal{V}_F$ . To facilitate the proof of the main results, for any  $q \in \mathcal{Q}$  and  $i \in \mathcal{V}_F$ , four quantities are introduced:

$$U_q(h) \triangleq e^{\text{Re}(\lambda_q)h} - \cos(\text{Im}(\lambda_q)h), \quad (6a)$$

$$V_q(h) \triangleq \sin(\text{Im}(\lambda_q)h), \quad (6b)$$

$$\phi_q(h) \triangleq \text{Arg}(U_q(h) + jV_q(h)), \quad (6c)$$

$$\psi_{i,q}(h) \triangleq \theta_i + \phi_q(h) - \theta_q. \quad (6d)$$

$\phi_q(h)$  is well-defined when  $U_q(h) + jV_q(h) \neq 0$ . If this is not the case, then  $\phi_q(h)$  will be determined through some limiting processes, e.g.,  $\lim_{h \rightarrow 0} \text{Arg}(U_q(h) + jV_q(h))$  or  $\lim_{\lambda_q \rightarrow 0} \text{Arg}(U_q(h) + jV_q(h))$ . The lemma below gives some important properties of these quantities, and its proof is provided in Appendix A.

*Lemma 1:* For  $U_q(h)$ ,  $V_q(h)$ ,  $\theta_q$ , and  $\phi_q(h)$  defined in (6), the following relationships hold:

- 1)  $\lim_{\lambda_q \rightarrow 0} \frac{V_q^2(h) + U_q^2(h)}{|\lambda_q|^2} = h^2$ ,
- 2)  $\lim_{\lambda_q \rightarrow 0} (\phi_q(h) - \theta_q) = 0$ ,
- 3)  $\lim_{h \rightarrow 0} \frac{U_q^2(h) + V_q^2(h)}{h^2} = |\lambda_q|^2$ ,
- 4)  $\lim_{h \rightarrow 0} (\phi_q(h) - \theta_q) = 0$ .

We end this section by presenting a technical lemma [36, Lemma 3.1], which will be used for stability analysis.

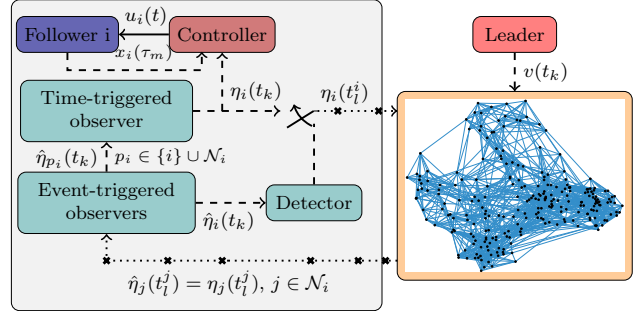


**Figure 1.** Schematic of mixed time- and event-triggered observers

*Lemma 2:* Consider the following discrete-time system

$$x(t_{k+1}) = Fx(t_k) + G(t_k),$$

where  $x(t_k) \in \mathbb{R}^n$ ,  $F \in \mathbb{R}^{n \times n}$ , and  $G(t_k) \in \mathbb{R}^n$ . Suppose that  $F$  is Schur and  $G(t_k)$  is well-defined. Then, if  $\lim_{t_k \rightarrow \infty} G(t_k) = 0$ ,  $\lim_{t_k \rightarrow \infty} x(t_k) = 0$  for any  $x(t_0) \in \mathbb{R}^n$ .

### III. DISTRIBUTED OBSERVER DESIGN

Our design schematic is shown in Figure 1, and the time-triggered observer and the event-triggered observer are introduced in the following.

#### A. Mixed time- and event-triggered observers

As the state of the leader is not assumed to be accessible to all the followers, we introduce the following time-triggered observer for each follower to estimate the state of the leader

$$\dot{\eta}_i(t) = S\eta_i(t) + \mu \sum_{j \in \mathcal{N}_i} (\hat{\eta}_j(t) - \hat{\eta}_i(t)), \quad (7)$$

where  $\mu > 0$  is the observer gain to be determined;  $\hat{\eta}_0(t) = v(t)$ ;  $\eta_i(t) \in \mathbb{R}^n$ ,  $i \in \mathcal{V}_F$ , is the estimation of  $v(t)$ ;  $\hat{\eta}_i(t)$  and  $\hat{\eta}_j(t)$ ,  $j \in \mathcal{N}_i$  are the auxiliary estimation signals of  $\eta_i(t)$  and  $\eta_j(t)$ ,  $j \in \mathcal{N}_i$ , respectively. For each follower  $i$ , the auxiliary estimation signals  $\hat{\eta}_{p_i}(t)$ ,  $p_i \in \{i\} \cup \mathcal{N}_i$ , are updated periodically with a step size  $h > 0$ , and the zero-order holder is used to maintain the signals between sampling instants, namely,

$$\hat{\eta}_{p_i}(t) = \hat{\eta}_{p_i}(t_k), \quad t \in [t_k, t_{k+1}), \quad k \in \mathbb{N},$$

$$h = t_{k+1} - t_k.$$

The discrete-time auxiliary estimation signals  $\hat{\eta}_{p_i}(t_k)$ ,  $p_i \in \{i\} \cup \mathcal{N}_i$ , of each follower  $i$  are generated by an auxiliary observer with event-triggered communication:

$$\hat{\eta}_{p_i}(t_{k+1}) = e^{Sh} \hat{\eta}_{p_i}(t_k), \quad t_k \neq t_l^{p_i}, \quad l \in \mathbb{Z}^+,$$

$$\hat{\eta}_{p_i}(t_l^{p_i}) = \eta_{p_i}(t_l^{p_i}), \quad t_k = t_l^{p_i}, \quad l \in \mathbb{Z}^+, \quad (8)$$

where  $t_l^{p_i}$  denotes the  $l$ -th triggering instant of follower  $p_i$ . Each follower  $i$  is equipped with such a time-triggered observer on  $\eta_i$  and an event-triggered observer on  $\eta_{p_i}$ ,  $p_i \in \{i\} \cup \mathcal{N}_i$ . At each triggering instant  $t_l^{p_i}$ , follower  $i$  broadcasts its estimation  $\eta_i(t_l^{p_i})$ , and related followers update their auxiliary observers accordingly. The sequence of triggering instants  $t_l^{p_i}$ ,

$l \in \mathbb{Z}^+$  for each follower  $i$  is generated by the following event-triggered mechanism

$$t_{l+1}^i = t_l^i + s_l^i h, \quad (9a)$$

$$s_l^i = \min \left\{ r \in \mathbb{Z}^+ \mid \left\| \bar{\eta}_i(t_k) \right\| > f_i(t_k), \right. \\ \left. t_k = t_l^i + r h. \right\}, \quad (9b)$$

where  $s_l^i$  is the inter-event step of follower  $i$ ;  $\bar{\eta}_i(t) \triangleq \eta_i(t) - \hat{\eta}_i(t)$  is the *absolute auxiliary error* of follower  $i$ ;  $f_i(t_k)$  for each  $i \in \mathcal{V}_F$  is a positive bounded function and *converges to zero* as  $t_k \rightarrow \infty$ , e.g.,  $f_i(t_k) = \frac{\sigma_i}{\alpha_i t_k + 1}$  or  $f_i(t_k) = \sigma_i \ln(1 + e^{-\alpha_i t_k})$ . With the mechanism in (9), triggering events only occur at sampling/updating instants, that is,  $\{t_0^i, t_1^i, \dots\} \subseteq \{t_0, t_1, t_2, \dots\}$ , and the set of inter-event time  $\{t_{l+1}^i - t_l^i, l \in \mathbb{Z}^+, i \in \mathcal{V}_F\}$  is lower bounded by the sampling period  $h$ .

Define the *estimation error* and the *relative auxiliary error* of follower  $i$  as  $\tilde{\eta}_i(t) \triangleq \eta_i(t) - v(t)$  and  $\hat{\eta}_{ei}(t) \triangleq \sum_{j \in \mathcal{N}_i} (\hat{\eta}_j(t) - \hat{\eta}_i(t))$ , respectively. Let  $\tilde{\eta} \triangleq \text{col}(\tilde{\eta}_1, \dots, \tilde{\eta}_N)$ ,  $\hat{\eta}_e \triangleq \text{col}(\hat{\eta}_{e1}, \dots, \hat{\eta}_{eN})$  and  $\bar{\eta} \triangleq \text{col}(\bar{\eta}_1, \dots, \bar{\eta}_N)$  denote the stacked versions of related signals. Then, the estimation error dynamics can be described by

$$\dot{\tilde{\eta}}(t) = (I_N \otimes S) \tilde{\eta}(t) + \mu \hat{\eta}_e(t_k), \quad t \in [t_k, t_{k+1}). \quad (10)$$

At each sampling instant, the stacked relative auxiliary error can be represented as

$$\hat{\eta}_e(t_k) = -(H \otimes I_n) (\bar{\eta}(t_k) - \bar{\eta}(t_k)). \quad (11)$$

Combining (10) and (11) yields a compact representation of the estimation error dynamics for  $t \in [t_k, t_{k+1})$  as follows

$$\dot{\tilde{\eta}}(t) = (I_N \otimes S) \tilde{\eta}(t) - \mu (H \otimes I_n) (\bar{\eta}(t_k) - \bar{\eta}(t_k)). \quad (12)$$

By applying the step-invariant transformation [12], the continuous-time system in (12) can be discretized to the system

$$\tilde{\eta}(t_{k+1}) = F(\mu) \tilde{\eta}(t_k) + G(\mu) \bar{\eta}(t_k), \quad (13)$$

where

$$F(\mu) = I_N \otimes e^{Sh} - \mu H \otimes \int_0^h e^{S\tau} d\tau, \\ G(\mu) = \mu H \otimes \int_0^h e^{S\tau} d\tau.$$

If events are triggered at all sampling instants, that is,  $s_l^i \equiv 1$ , then  $\bar{\eta}(t_k) \equiv 0$ , and (13) reduces to the following purely time-triggered error dynamic system

$$\tilde{\eta}(t_{k+1}) = F(\mu) \tilde{\eta}(t_k). \quad (14)$$

### B. Stability of the time-triggered error dynamics

To drive the estimation error  $\tilde{\eta}(t_k)$  in (13) to zero as time tends to infinity, the stability of the time-triggered error dynamics in (14) is critical. The following lemma gives a necessary and sufficient condition for the stability of (14) and reveals some fundamental relationships among sampling periods, topologies, and reference signals.

**Lemma 3:** Under Assumption 3, there exists a  $\mu > 0$  such that  $F(\mu)$  is Schur if and only if  $h$  satisfies the conditions below:

(I) Phase condition:

$$\psi_{i,q}(h) \in \left(-\frac{\pi}{2}, \frac{\pi}{2}\right), \quad q \in \mathcal{Q}_1 \cup \mathcal{Q}_3 \quad \text{and} \quad i \in \mathcal{V}_F;$$

(II) Magnitude condition:

$$e^{2\text{Re}(\lambda_q)h} < \csc^2 \psi_{i,q}(h), \quad q \in \mathcal{Q}_1 \quad \text{and} \quad i \in \mathcal{V}_F;$$

(III) Non-zero spectral mapping:

$$h \neq \frac{2\kappa\pi}{\text{Im}(\lambda_q)}, \quad q \in \mathcal{Q}_3 \quad \text{and} \quad i \in \mathcal{V}_F,$$

where  $\kappa \in \mathbb{Z}$  and  $\frac{\kappa}{\text{Im}(\lambda_q)} > 0$ ;

(IV)  $\bigcap_{q \in \mathcal{Q}, i \in \mathcal{V}_F} (\underline{\mu}_{i,q}, \bar{\mu}_{i,q}) \neq \emptyset$ ,

where

$$\bar{\mu}_{i,q} = \frac{|\lambda_q|}{|\lambda_i|} \frac{\cos(\psi_{i,q}(h)) + \sqrt{e^{-2\text{Re}(\lambda_q)h} - \sin^2(\psi_{i,q}(h))}}{e^{\text{Re}(-\lambda_q)h} \sqrt{V_q^2(h) + U_q^2(h)}}, \\ \underline{\mu}_{i,q} = \frac{|\lambda_q|}{|\lambda_i|} \frac{\cos(\psi_{i,q}(h)) - \sqrt{e^{-2\text{Re}(\lambda_q)h} - \sin^2(\psi_{i,q}(h))}}{e^{\text{Re}(-\lambda_q)h} \sqrt{V_q^2(h) + U_q^2(h)}}. \quad (15)$$

*Proof:* It can be verified from the property of Kronecker product and the spectral mapping theorem that the eigenvalues of  $F(\mu)$  are given by:

$$e^{\lambda_q h} - \mu \lambda_i \int_0^h e^{\lambda_q \tau} d\tau, \quad q \in \mathcal{Q} \quad \text{and} \quad i \in \mathcal{V}_F.$$

Obviously,  $F(\mu)$  is Schur if and only if these eigenvalues are in the unit circle. Direct calculation gives that

$$|e^{\lambda_q h} - \mu \lambda_i \int_0^h e^{\lambda_q \tau} d\tau|^2 - 1 = \alpha_{i,q} \mu^2 + \beta_{i,q} \mu + \gamma_{i,q},$$

where

$$\alpha_{i,q} = |\lambda_i|^2 \left| \int_0^h e^{\lambda_q \tau} d\tau \right|^2, \\ \beta_{i,q} = -2 \text{Re}(\lambda_i) \int_0^h e^{\lambda_q \tau + \lambda_i^* h} d\tau, \quad (16) \\ \gamma_{i,q} = |e^{\lambda_q h}|^2 - 1, \quad q \in \mathcal{Q} \quad \text{and} \quad i \in \mathcal{V}_F.$$

Hence,  $F(\mu)$  is Schur if and only if there exists a  $\mu > 0$  such that  $\alpha_{i,q} \mu^2 + \beta_{i,q} \mu + \gamma_{i,q} < 0$  for all possible  $i$  and  $q$ . For any  $q \in \mathcal{Q}_1 \cup \mathcal{Q}_2 \cup \mathcal{Q}_3$  and  $i \in \mathcal{V}_F$ , we have that (see Appendix B for the derivations)

$$\alpha_{i,q} = \frac{|\lambda_i|^2}{|\lambda_q|^2} (U_q^2(h) + V_q^2(h)), \\ \beta_{i,q} = -2 \frac{|\lambda_i|}{|\lambda_q|} e^{\text{Re}(\lambda_q)h} \sqrt{V_q^2(h) + U_q^2(h)} \cos(\psi_{i,q}(h)), \quad (17) \\ \gamma_{i,q} = e^{2\text{Re}(\lambda_q)h} - 1.$$

For  $q \in \mathcal{Q}_4$  and  $i \in \mathcal{V}_F$ ,  $\lambda_q = 0$ , which implies that  $\alpha_{i,q} = |\lambda_i|^2 h^2$ ,  $\beta_{i,q} = -2h \text{Re}(\lambda_i)$  and  $\gamma_{i,q} = 0$  from (16). It can be evaluated from Lemma 1 that

$$\alpha_{i,q} = \lim_{\lambda_q \rightarrow 0} \frac{|\lambda_i|^2}{|\lambda_q|^2} (U_q^2(h) + V_q^2(h)) = |\lambda_i|^2 h^2, \\ \beta_{i,q} = -2|\lambda_i| \lim_{\lambda_q \rightarrow 0} \frac{\sqrt{V_q^2(h) + U_q^2(h)}}{|\lambda_q|} e^{\text{Re}(\lambda_q)h} \cos(\psi_{i,q}(h))$$

$$= -2h\text{Re}(\lambda_i),$$

$$\gamma_{i,q} = \lim_{\lambda_q \rightarrow 0} e^{2\text{Re}(\lambda_q)h} - 1 = 0.$$

Therefore, for any  $q \in \mathcal{Q}$  and  $i \in \mathcal{V}_F$ ,  $\alpha_{i,q}$ ,  $\beta_{i,q}$  and  $\gamma_{i,q}$  can be expressed by (17). Based on the partition in (5) and the coefficients in (17), the existence of  $\mu > 0$  is discussed below.

**Case 1.**  $q \in \mathcal{Q}_1$  and  $i \in \mathcal{V}_F$ :

As  $\text{Re}(\lambda_q) > 0$ ,  $|e^{\lambda_q h}| = |e^{\text{Re}(\lambda_q)h}| > 1$ , which implies  $\gamma_{i,q} > 0$ . Noting that  $U_q(h)$  in (6) cannot be zero for any  $q \in \mathcal{Q}_1$ , we have that  $\alpha_{i,q} > 0$ . Since  $\gamma_{i,q} > 0$  and  $\alpha_{i,q} > 0$ , there exists a  $\mu > 0$  such that  $\alpha_{i,q}\mu^2 + \beta_{i,q}\mu + \gamma_{i,q} < 0$  if and only if  $\beta_{i,q} < 0$  and  $\beta_{i,q}^2 - 4\alpha_{i,q}\gamma_{i,q} > 0$ , which is equivalent to  $\cos(\psi_{i,q}(h)) > 0$  and  $1 - e^{2\text{Re}(\lambda_q)h} \sin^2(\psi_{i,q}(h)) > 0$  from the derivations in Appendix B. Hence, there exists a  $\mu > 0$  such that  $\alpha_{i,q}\mu^2 + \beta_{i,q}\mu + \gamma_{i,q} < 0$  if and only if the following two conditions are satisfied

- (a)  $2\kappa\pi - \frac{\pi}{2} < \psi_{i,q}(h) < 2\kappa\pi + \frac{\pi}{2}$ ,  $\kappa \in \mathbb{Z}$ ,
- (b)  $e^{2\text{Re}(\lambda_q)h} < \csc^2 \psi_{i,q}(h)$ .

Owing to  $\text{Re}(\lambda_q) > 0$ ,  $\theta_q \in (-\frac{1}{2}\pi, \frac{1}{2}\pi)$  and  $U_q(h) > 0$ , it follows that  $\phi_q(h) \in (-\frac{1}{2}\pi, \frac{1}{2}\pi)$  from (6). Under Assumption 3, all eigenvalues of  $H$  have positive real parts, which leads to  $\theta_i \in (-\frac{1}{2}\pi, \frac{1}{2}\pi)$ . As a result,  $\psi_{i,q}(h) \in (-\frac{3}{2}\pi, \frac{3}{2}\pi)$ . Accordingly, condition (a) reduces to  $-\frac{\pi}{2} < \psi_{i,q}(h) < \frac{\pi}{2}$ .

**Case 2.**  $q \in \mathcal{Q}_2$  and  $i \in \mathcal{V}_F$ :

As  $\text{Re}(\lambda_q) < 0$ ,  $|e^{\lambda_q h}| = |e^{\text{Re}(\lambda_q)h}| < 1$ , which implies that  $\gamma_{i,q} < 0$ . It follows from (6) that  $U_q(h)$  and  $V_q(h)$  cannot be equal to zero when  $q \in \mathcal{Q}_2$ , and thus  $\alpha_{i,q} > 0$ . Since  $\alpha_{i,q} > 0$  and  $\gamma_{i,q} < 0$ , there exists a  $\mu > 0$  such that  $\alpha_{i,q}\mu^2 + \beta_{i,q}\mu + \gamma_{i,q} < 0$  if and only if  $\beta_{i,q}^2 - 4\alpha_{i,q}\gamma_{i,q} > 0$ , which is equivalent to  $e^{2\text{Re}(\lambda_q)h} < \csc^2 \psi_{i,q}(h)$  from the derivations in Appendix B. It is noted that

$$\sin^2(\psi_{i,q}(h)) < 1 < e^{-2\text{Re}(\lambda_q)h}, \text{ for any } q \in \mathcal{Q}_2.$$

Hence, the condition  $e^{2\text{Re}(\lambda_q)h} < \csc^2 \psi_{i,q}(h)$  always holds, and there exists a  $\mu > 0$  such that  $\alpha_{i,q}\mu^2 + \beta_{i,q}\mu + \gamma_{i,q} < 0$  for any  $q \in \mathcal{Q}_2$  and  $h > 0$ .

**Case 3.**  $q \in \mathcal{Q}_3$  and  $i \in \mathcal{V}_F$ :

As  $\text{Re}(\lambda_q) = 0$ ,  $|e^{\lambda_q h}| = |e^{\text{Re}(\lambda_q)h}| = 1$ , which yields that  $\gamma_{i,q} = 0$ . There exists a  $\mu > 0$  such that  $\alpha_{i,q}\mu^2 + \beta_{i,q}\mu < 0$  if and only if  $\beta_{i,q} < 0$ , which is equivalent to  $\cos(\psi_{i,q}(h)) > 0$  and  $\sqrt{V_q^2(h) + U_q^2(h)} \neq 0$  from (17). Hence, there exists a  $\mu > 0$  such that  $\alpha_{i,q}\mu^2 + \beta_{i,q}\mu < 0$  if and only if  $h$  satisfies

- (a)  $2\kappa\pi - \frac{\pi}{2} < \psi_{i,q}(h) < 2\kappa\pi + \frac{\pi}{2}$ ,  $\kappa \in \mathbb{Z}$ ,
- (b)  $\text{Im}(\lambda_q)h \neq 2\kappa\pi$ ,  $\kappa \in \mathbb{Z}$ .

When  $\text{Im}(\lambda_q)h = 2\kappa\pi$ ,  $U_q(h) = V_q(h) = 0$ , and  $\phi_q(h)$  can be determined by using the limiting process, that is,  $\phi_q(h) = \pm\frac{\pi}{2}$ . Otherwise,  $U_q(h) > 0$ , which implies that  $\phi_q(h) \in (-\frac{1}{2}\pi, \frac{1}{2}\pi)$ . Hence,  $\phi_q(h) \in [-\frac{1}{2}\pi, \frac{1}{2}\pi]$ . Under Assumption 3, all eigenvalues of  $H$  have positive real parts, which lead to  $\theta_i \in (-\frac{1}{2}\pi, \frac{1}{2}\pi)$ . Also, it follows from  $\text{Re}(\lambda_q) = 0$  that  $\theta_q = \pm\frac{\pi}{2}$ . Therefore,  $\psi_{i,q}(h) \in (-\frac{3}{2}\pi, \frac{3}{2}\pi)$ , and condition (a) reduces to  $-\frac{\pi}{2} < \psi_{i,q}(h) < \frac{\pi}{2}$ . Regarding condition (b), it reduces to  $h \neq \frac{2\kappa\pi}{\text{Im}(\lambda_q)}$ ,  $\frac{\kappa}{\text{Im}(\lambda_q)} > 0$ , since  $h$  is positive.

**Case 4.**  $q \in \mathcal{Q}_4$  and  $i \in \mathcal{V}_F$ :

For  $q \in \mathcal{Q}_4$ ,  $\lambda_q = 0$  implies  $\alpha_{i,q} = |\lambda_i|^2 h^2$ ,  $\beta_{i,q} = -2h\text{Re}(\lambda_i)$  and  $\gamma_{i,q} = 0$  from (16). Under Assumption 3, all eigenvalues

of  $H$  have positive real parts and  $h > 0$ , which leads to  $\beta_{i,q} < 0$  and  $\alpha_{i,q} > 0$ . Thus,  $\alpha_{i,q}\mu^2 + \beta_{i,q}\mu < 0$  always has positive solutions for any  $q \in \mathcal{Q}_4$  and  $h > 0$ .

Next, we show that for each  $q \in \mathcal{Q}$ , the solutions of  $\alpha_{i,q}\mu^2 + \beta_{i,q}\mu + \gamma_{i,q} = 0$  can be represented by (15). For any  $q \in \mathcal{Q}_1 \cup \mathcal{Q}_2 \cup \mathcal{Q}_3$  and  $i \in \mathcal{V}_F$ , it is easy to verify that the roots of  $\alpha_{i,q}\mu^2 + \beta_{i,q}\mu + \gamma_{i,q} = 0$  are  $\bar{\mu}_{i,q}$  and  $\underline{\mu}_{i,q}$  in (15). Under Assumption 3, all eigenvalues of  $H$  have positive real parts, that is,  $\cos(\theta_i) = \frac{\text{Re}(\lambda_i)}{|\lambda_i|} > 0$ . By using Lemma 1, for the  $\bar{\mu}_{i,q}$  and  $\underline{\mu}_{i,q}$  defined in (15), we have that

$$\lim_{\lambda_q \rightarrow 0} \bar{\mu}_{i,q} = \frac{1}{|\lambda_i|} \frac{\cos(\theta_i) + |\cos(\theta_i)|}{h} = \frac{2\text{Re}(\lambda_i)}{|\lambda_i|^2 h},$$

$$\lim_{\lambda_q \rightarrow 0} \underline{\mu}_{i,q} = \frac{1}{|\lambda_i|} \frac{\cos(\theta_i) - |\cos(\theta_i)|}{h} = 0. \quad (18)$$

In addition, for  $q \in \mathcal{Q}_4$  and  $i \in \mathcal{V}_F$ , the roots of  $\alpha_{i,q}\mu^2 + \beta_{i,q}\mu + \gamma_{i,q} = 0$  are

$$\underline{\mu}_{i,q} = 0 \text{ and } \bar{\mu}_{i,q} = \frac{2\text{Re}(\lambda_i)}{|\lambda_i|^2 h}, \quad (19)$$

respectively. Hence, the equations in (15) are equivalent to the equations in (19) when  $q \in \mathcal{Q}_4$  because of (18). In conclusion,  $\mu > 0$  exists if and only if conditions (I) to (IV) are all satisfied.  $\square$

*Remark 1:* Lemma 3 gives all feasible sampling periods that leads to convergent error dynamics and observable connected systems. This can be regarded as an extension of the non-pathological sampling periods for observability in [12] to distributed systems.

A significant feature of the distributed system considered in this paper is that the observability under sampling is related not only to the system dynamics but also to the topological connection. According to Lemma 1 and (6),  $\lim_{h \rightarrow 0} \frac{U_q(h) + jV_q(h)}{h\lambda_q} =$

1. In terms of this,  $\frac{U_q(h) + jV_q(h)}{h}$  can be regarded as the sampled version of  $\lambda_q$  with the proposed distributed observers, and  $\phi_q(h) - \theta_q$  is the phase shift of  $\lambda_q$  due to sampling. These phase shifts of the eigenvalues of  $S$  and the phases  $\theta_i$  related to the graph jointly determine the observability as shown in condition (I). Also, condition (II) manifests that the sampling period  $h$  cannot be too large. Besides, to guarantee the observability, the sampled eigenvalues  $\frac{U_q(h) + jV_q(h)}{h}$  as revealed in condition (III) must be non-zero, which corresponds to the temporal anti-aliasing of signals, and this is consistent with the centralized control and signal processing.

The following corollary shows that Lemma 3 includes the result in [8] as a special case.

*Corollary 1:* For  $i \in \mathcal{V}_F$  and  $q \in \mathcal{Q}$ ,  $\lim_{h \rightarrow 0} \bar{\mu}_{i,q} = +\infty$ ,  $\lim_{h \rightarrow 0} \underline{\mu}_{i,q} = \frac{\text{Re}(\lambda_q)}{\text{Re}(\lambda_i)}$ , and

$$\lim_{h \rightarrow 0} \bigcap_{q \in \mathcal{Q}, i \in \mathcal{V}_F} (\underline{\mu}_{i,q}, \bar{\mu}_{i,q}) = \left( \frac{\max_{q \in \mathcal{Q}} (\text{Re}(\lambda_q))}{\min_{i \in \mathcal{V}_F} (\text{Re}(\lambda_i))}, +\infty \right)$$

where  $\bar{\mu}_{i,q}$  and  $\underline{\mu}_{i,q}$  are defined in (15).

*Proof:* It follows from Lemma 1 and Appendix B that

$$\lim_{h \rightarrow 0} \frac{\alpha_{i,q}}{h} = \lim_{h \rightarrow 0} \frac{|\lambda_i|^2 V_q^2(h) + U_q^2(h)}{|\lambda_q|^2 h} = 0, \quad (20a)$$

$$\lim_{h \rightarrow 0} \frac{\beta_{i,q}}{h} = -2\text{Re}(\lambda_i), \quad (20b)$$

$$\lim_{h \rightarrow 0} \frac{\gamma_{i,q}}{h} = 2\text{Re}(\lambda_q). \quad (20c)$$

where  $\alpha_{i,q}$ ,  $\beta_{i,q}$ , and  $\gamma_{i,q}$  are defined in (16). For  $i \in \mathcal{V}_F$  and  $q \in \mathcal{Q}$ , the solutions to  $\alpha_{i,q}\mu^2 + \beta_{i,q}\mu + \gamma_{i,q} = 0$  are given by  $\bar{\mu}_{i,q} = \frac{-\beta_{i,q} + \sqrt{\beta_{i,q}^2 - 4\alpha_{i,q}\gamma_{i,q}}}{2\alpha_{i,q}}$  and  $\underline{\mu}_{i,q} = \frac{-\beta_{i,q} - \sqrt{\beta_{i,q}^2 - 4\alpha_{i,q}\gamma_{i,q}}}{2\alpha_{i,q}}$ , respectively. Under Assumption 3, all eigenvalues of  $H$  have positive real parts, which leads to  $\lim_{h \rightarrow 0} \sqrt{\frac{\beta_{i,q}^2}{h^2} - 4\frac{\alpha_{i,q}\gamma_{i,q}}{h^2}} = 2\text{Re}(\lambda_i)$ . Based on this and (20), we have that

$$\begin{aligned} \lim_{h \rightarrow 0} \bar{\mu}_{i,q} &= \lim_{h \rightarrow 0} \frac{-\beta_{i,q}/h + \sqrt{\beta_{i,q}^2 - 4\alpha_{i,q}\gamma_{i,q}}/h}{2\alpha_{i,q}/h} \\ &= \frac{4\text{Re}(\lambda_i)}{0} \\ &= +\infty \end{aligned}$$

and

$$\begin{aligned} \lim_{h \rightarrow 0} \underline{\mu}_{i,q} &= \lim_{h \rightarrow 0} \frac{2\gamma_{i,q}}{-\beta_{i,q} + \sqrt{\beta_{i,q}^2 - 4\alpha_{i,q}\gamma_{i,q}}} \\ &= \lim_{h \rightarrow 0} \frac{2\gamma_{i,q}/h}{-\beta_{i,q}/h + \sqrt{\beta_{i,q}^2 - 4\alpha_{i,q}\gamma_{i,q}}/h} \\ &= \frac{\text{Re}(\lambda_q)}{\text{Re}(\lambda_i)}. \end{aligned}$$

Finally,  $\lim_{h \rightarrow 0} \bigcap_{q \in \mathcal{Q}} \bigcap_{i \in \mathcal{V}_F} (\underline{\mu}_{i,q}, \bar{\mu}_{i,q}) = (\frac{\max_{q \in \mathcal{Q}}(\text{Re}(\lambda_q))}{\min_{i \in \mathcal{V}_F}(\text{Re}(\lambda_i))}, +\infty)$ . This completes the proof.  $\square$

On the one hand, the observer gain  $\mu$  for the continuous-time distributed observer proposed in [8] should be selected as an arbitrarily large value such that  $\mu \in (\frac{\max_{q \in \mathcal{Q}}(\text{Re}(\lambda_q))}{\min_{i \in \mathcal{V}_F}(\text{Re}(\lambda_i))}, +\infty)$  (See the proof of (author?) [8, Theorem 1]). Clearly, Corollary 1 directly shows that Lemma 3 includes the result in [8] as a special case when  $h \rightarrow 0$ . Furthermore, in our time-triggered distributed observer,  $\mu$  cannot be selected arbitrarily, as revealed in Lemma 3, due to the interaction among sampling periods, topologies, and the system dynamics. Instead, to generate convergent error dynamics,  $\mu$  needs to be designed deliberately by considering the interaction.

On the other hand, in the existing literature, the sampling period  $h$  is usually selected as a sufficiently small number or restricted to some values on a fixed interval governed by linear matrix inequalities or the spectral radius/norm of certain graph induced matrix, e.g., [37] and [30]. By contrast, a complete characterization of all possible sampling periods and their impact on the observability of the connected systems has been given in Lemma 3. In the following corollary, explicit feasible sampling periods are further provided when the reference signal is a sinusoidal wave.

*Corollary 2:* Under Assumption 3 and  $\mathcal{Q} = \mathcal{Q}_3$ , there exists a  $\mu$  such that  $F(\mu)$  is Schur if and only if  $h$  satisfies the following conditions for  $q \in \mathcal{Q}$  and  $\kappa \in \mathbb{Z}^+$ :

$$\begin{cases} 2\kappa\pi - 2\pi < |\text{Im}(\lambda_q)|h < 2\kappa\pi, \\ 2\kappa\pi - 3\pi + 2\theta_i < |\text{Im}(\lambda_q)|h < 2\kappa\pi - \pi + 2\theta_i, \\ 2\kappa\pi - 3\pi - 2\theta_i < |\text{Im}(\lambda_q)|h < 2\kappa\pi - \pi - 2\theta_i. \end{cases}$$

*Proof:* For  $q \in \mathcal{Q} = \mathcal{Q}_3$ ,  $\text{Re}(\lambda_q) = 0$  implies  $\theta_q = \pm \frac{\pi}{2}$ ,  $U_q(h) = 1 - \cos(\text{Im}(\lambda_q)h)$ , and  $V_q(h) = \sin(\text{Im}(\lambda_q)h)$ . Then, it follows from Lemma 3 that there exists a  $\mu$  such that  $F(\mu)$  is Schur if and only if

$$\begin{cases} |\text{Im}(\lambda_q)|h \neq 2\kappa_1\pi, & \kappa_1 \in \mathbb{Z}^+ \\ 0 < \phi_q(h) + \theta_i < \pi, & \text{when } \theta_q = \frac{\pi}{2}, \\ -\pi < \phi_q(h) + \theta_i < 0, & \text{when } \theta_q = -\frac{\pi}{2}. \end{cases}$$

Since  $U_q > 0$  under these conditions, we have that  $\phi_q(h) \in (-\frac{\pi}{2}, \frac{\pi}{2})$  and

$$\begin{aligned} \phi_q(h) &= \arctan \frac{V_q(h)}{U_q(h)} \\ &= \arctan \frac{\sin(\text{Im}(\lambda_q)h)}{1 - \cos(\text{Im}(\lambda_q)h)} \\ &= \arctan \left[ \cot\left(\frac{\text{Im}(\lambda_q)}{2}h\right) \right] \\ &= \arctan \left[ \tan\left(\kappa\pi + \frac{\pi}{2} - \frac{\text{Im}(\lambda_q)}{2}h\right) \right], \quad \kappa \in \mathbb{Z}, \quad (21) \end{aligned}$$

which further lead to

$$\begin{cases} -\frac{\pi}{2} < \kappa_2\pi + \frac{\pi}{2} - \frac{|\text{Im}(\lambda_q)|}{2}h < \frac{\pi}{2}, & \theta_q = \frac{\pi}{2}, \quad \kappa_2 \in \mathbb{Z}, \\ 0 < \kappa_2\pi + \frac{\pi}{2} - \frac{|\text{Im}(\lambda_q)|}{2}h + \theta_i < \pi, & \end{cases}$$

and

$$\begin{cases} -\frac{\pi}{2} < \kappa_3\pi + \frac{\pi}{2} + \frac{|\text{Im}(\lambda_q)|}{2}h < \frac{\pi}{2}, & \theta_q = -\frac{\pi}{2}, \quad \kappa_3 \in \mathbb{Z}. \\ -\pi < \kappa_3\pi + \frac{\pi}{2} + \frac{|\text{Im}(\lambda_q)|}{2}h + \theta_i < 0, & \end{cases}$$

Through some simple algebraic manipulations, these two conditions can be further simplified to (1) for  $\theta_q = \frac{\pi}{2}$  and  $\kappa_2 \in \{0, 1, 2, \dots\}$ ,

$$\begin{cases} 2\kappa_2\pi < |\text{Im}(\lambda_q)|h < 2\kappa_2\pi + 2\pi, \\ 2\kappa_2\pi - \pi + 2\theta_i < |\text{Im}(\lambda_q)|h < 2\kappa_2\pi + \pi + 2\theta_i, \end{cases}$$

and (2) for  $\theta_q = -\frac{\pi}{2}$  and  $\kappa_3 \in \{-1, -2, \dots\}$ ,

$$\begin{cases} -2\kappa_3\pi - 2\pi < |\text{Im}(\lambda_q)|h < -2\kappa_3\pi, \\ -2\kappa_3\pi - 3\pi - 2\theta_i < |\text{Im}(\lambda_q)|h < -2\kappa_3\pi - \pi - 2\theta_i. \end{cases}$$

It is obvious that conditions (1) and (2) naturally include the condition  $|\text{Im}(\lambda_q)|h \neq 2\kappa_1\pi$ ,  $\kappa_1 \in \mathbb{Z}^+$ , and are equivalent to the conditions in (2). This completes the proof.  $\square$

### C. Convergence of the mixed time- and event-triggered observers

Regarding the convergence of the estimation errors  $\tilde{\eta}_i$  with the triggering function in (9), we have the following theorem.

*Theorem 1:* Under Assumption 3, there exists a  $\mu > 0$  such that the estimation error  $\tilde{\eta}(t)$  of the mixed time- and event-triggered distributed observer converges for any event-triggered mechanism in the form of (9) if and only if  $h$  satisfies the conditions in Lemma 3. Furthermore, all feasible  $\mu > 0$  are in the set  $\bigcap_{q \in \mathcal{Q}} \bigcap_{i \in \mathcal{V}_F} (\underline{\mu}_{i,q}, \bar{\mu}_{i,q})$ , where  $\underline{\mu}_{i,q}$  and  $\bar{\mu}_{i,q}$  are defined in (15).

*Proof:* If  $h$  satisfies the conditions in Lemma 3, then, from Lemma 3, there exists a  $\mu \in \bigcap_{q \in \mathcal{Q}} \bigcap_{i \in \mathcal{V}_F} (\underline{\mu}_{i,q}, \bar{\mu}_{i,q})$  such that  $F(\mu)$  is Schur. The triggering function in (9) enforces  $\|\tilde{\eta}(t_k)\| \leq \sqrt{N}f(t_k)$  after applying the updating law in (8),

where  $f(t_k) = \max \{f_1(t_k), \dots, f_N(t_k)\}$ . Based on this and the convergence of  $f_i(t_k)$ , we have that

$$\lim_{t_k \rightarrow \infty} \bar{\eta}(t_k) = 0. \quad (22)$$

Applying Lemma 2 together with this to (13) yields that

$$\lim_{t_k \rightarrow \infty} \tilde{\eta}(t_k) = 0. \quad (23)$$

Then, from equation (12), we have that,  $\forall t \in [t_k, t_{k+1})$ ,

$$\|\tilde{\eta}(t)\| \leq e^{\|S\|h} [(1 + \mu h \|H\|) \|\tilde{\eta}(t_k)\| + \mu h \|H\| \|\tilde{\eta}(t_k)\|].$$

Therefore, it follows from (22) and (23) that  $\lim_{t \rightarrow \infty} \tilde{\eta}(t) = 0$ .

On the contrary, if  $\lim_{t \rightarrow \infty} \tilde{\eta}(t) = 0$ , then  $F(\mu)$  must be Schur, and thus  $h$  satisfies the conditions in Lemma 3.  $\square$

#### D. Inter-event analysis

Under Assumption 3, there exists a  $\mu$  such that  $F(\mu)$  is Schur for any  $h$  satisfying the conditions in Lemma 3. For such a matrix, there are constants  $\beta(h, \mu) > 0$  and  $0 \leq \gamma(h, \mu) < 1$  such that  $\|F^k(\mu)\| \leq \beta(h, \mu) \gamma^k(h, \mu)$ , where  $\gamma(h, \mu)$  is the spectral radius of  $F(\mu)$ . In the remaining analysis,  $\mu$  is supposed to be fixed, and  $h$  and  $\mu$  in  $\beta(h, \mu)$  and  $\gamma(h, \mu)$  are omitted for notational simplicity. To analyze the number of steps between two consecutive triggering instants, the triggering function for each follower  $i$  is assumed to be bounded by exponential functions, that is,

$$\sigma_m e^{-\alpha t_k} \leq f_i(t_k) \leq \sigma_M e^{-\alpha t_k}, \quad (24)$$

where  $\sigma_m > 0$ ,  $\sigma_M > 0$ , and  $\alpha > 0$ , for  $i \in \mathcal{V}_F$ . Given the triggering instant  $t_l^i$ , suppose that the next triggering instant is  $t_k = t_l^i + s_l^i h$ . Then, the solution of the system in (7) during the time interval  $[t_l^i, t_l^i + s_l^i h)$  can be evaluated as

$$\eta_i(t_k) = e^{S s_l^i h} \eta_i(t_l^i) + \mu \sum_{r=1}^{s_l^i} \int_{t_{k-r}}^{t_{k-r+1}} e^{S(t_k-\tau)} \hat{\eta}_{ei}(t_{k-r}) d\tau.$$

Consider equation (8) during the time interval  $[t_l^i, t_l^i + s_l^i h)$ . Then, we have that

$$\begin{aligned} \bar{\eta}_i(t_k^-) &= e^{S s_l^i h} \bar{\eta}_i(t_l^i) \\ &+ \mu \sum_{r=1}^{s_l^i} \int_{t_{k-r}}^{t_{k-r+1}} e^{S(t_k-\tau)} \hat{\eta}_{ei}(t_{k-r}) d\tau. \end{aligned} \quad (25)$$

where  $\bar{\eta}_i(t_k^-)$  denotes the value of  $\bar{\eta}_i(t)$  at  $t_k$  before applying the updating law in (8). In the following theorem, we establish a relationship among the inter-event steps  $s_l^i$ , the sampling period  $h$ , and the decay rate of the bounding functions  $\alpha$ . Before proceeding, we define some variables below

$$\begin{aligned} \chi_1 &\triangleq \mu \|H\| \sqrt{N} \sigma_M, & \chi_2(h) &\triangleq \frac{\chi_1 \beta \|G(\mu)\| e^{\alpha h}}{1 - \gamma e^{\alpha h}}, \\ \chi_3(k, h) &\triangleq \mu \|H\| \beta \|\tilde{\eta}(t_0)\| (\gamma e^{\alpha h})^k + \chi_2(h) [1 - (\gamma e^{\alpha h})^k]. \end{aligned}$$

**Theorem 2:** Under Assumption 3,  $s_l^i$  has the following properties for any event-triggered mechanism in the form of (9) with the triggering function in (24):

1) (Time-varying bound) there exists a positive  $s(k, h)$  such that

$$s_l^i > s(k, h), \quad k \in \mathbb{N}; \quad (26)$$

2) (Asymptotic bound) there exists a positive constant  $s^*(h)$  such that

$$\lim_{k \rightarrow \infty} s(k, h) = \begin{cases} s^*(h), & e^{\alpha h} \gamma < 1, \\ 0, & e^{\alpha h} \gamma \geq 1, \end{cases} \quad (27)$$

where  $s(k, h)$  and  $s^*(h)$  are given by the following equations in  $s$  and  $s^*$ , respectively,

$$\frac{e^{\|S\|sh} - 1}{\|S\|} = \frac{\sigma_m}{\gamma^{-s} \chi_3(k, h) + \chi_1 e^{\alpha hs}}, \quad (28a)$$

$$\frac{e^{\|S\|s^*h} - 1}{\|S\|} = \frac{\sigma_m}{\gamma^{-s^*} \chi_2(h) + \chi_1 e^{\alpha hs^*}}. \quad (28b)$$

*Proof:* Simple calculation from (13) gives that

$$\|\tilde{\eta}(t_k)\| \leq \beta \gamma^k \|\tilde{\eta}(t_0)\| + \sum_{r=0}^{k-1} \beta \gamma^{k-r-1} \|G(\mu)\| \|\tilde{\eta}(t_r)\|.$$

The event-triggered mechanism in (9) enforces  $\|\tilde{\eta}(t_r)\| \leq \sqrt{N} \sigma_M e^{-\alpha hr}$  after applying the updating law in (8). Then,

$$\|\tilde{\eta}(t_k)\| \leq \beta \gamma^k \|\tilde{\eta}(t_0)\| + \beta \sigma_M \sqrt{N} \|G(\mu)\| \gamma^{k-1} \sum_{r=0}^{k-1} \frac{e^{-\alpha hr}}{\gamma^r}$$

From equations (11), it follows that

$$\|\hat{\eta}_{ei}(t_k)\| \leq \|\hat{\eta}_e(t_k)\| \leq \|H\| (\|\tilde{\eta}(t_k)\| + \|\bar{\eta}(t_k)\|). \quad (29)$$

Obviously,  $\bar{\eta}_i(t_l^i) = 0$ , which implies together with (25) that

$$\bar{\eta}_i(t_k^-) = \mu \sum_{r=1}^{s_l^i} \int_{t_{k-r}}^{t_{k-r+1}} e^{S(t_k-\tau)} \hat{\eta}_{ei}(t_{k-r}) d\tau. \quad (30)$$

For any positive  $r \leq s_l^i$ , it is noted that  $\gamma^{k-r-1} \leq \gamma^{k-s_l^i-1}$ ,  $\gamma^{k-r} \leq \gamma^{k-s_l^i}$ , and  $\sum_{v=0}^{k-r-1} \frac{e^{-\alpha hv}}{\gamma^v} \leq \sum_{v=0}^{k-1} \frac{e^{-\alpha hv}}{\gamma^v}$ . Then, from equations (29), (30), and  $\|\bar{\eta}(t_r)\| \leq \sqrt{N} \sigma_M e^{-\alpha hr}$ , it follows that

$$\begin{aligned} \|\bar{\eta}_i(t_k^-)\| &\leq \mu \sum_{r=1}^{s_l^i} \int_{t_{k-r}}^{t_{k-r+1}} \|e^{S(t_k-\tau)}\| \|\hat{\eta}_e(t_{k-r})\| d\tau \\ &\leq \int_0^{s_l^i h} \|e^{S\tau}\| d\tau [\gamma^{-s_l^i} \chi_3(k, h) + \chi_1 e^{\alpha h s_l^i}] e^{-\alpha h k} \\ &\leq \int_0^{s_l^i h} e^{\|S\|\tau} d\tau [\gamma^{-s_l^i} \chi_3(k, h) + \chi_1 e^{\alpha h s_l^i}] e^{-\alpha h k}. \end{aligned} \quad (31)$$

On the other hand,

$$\|\bar{\eta}_i(t_k^-)\| = \|\bar{\eta}_i(t_l^i + s_l^i h)\| > f_i(t_k) \geq \sigma_m e^{-\alpha h k}. \quad (32)$$

Combining (31) and (32) yields that

$$\frac{e^{\|S\|s_l^i h} - 1}{\|S\|} > \frac{\sigma_m}{\gamma^{-s_l^i} \chi_3(k, h) + \chi_1 e^{\alpha h s_l^i}}, \quad \|S\| \neq 0, \quad (33)$$

When  $\|S\| = 0$ , it is easy to show the left side of (33) can be evaluated using the limiting process  $\lim_{\|S\| \rightarrow 0} \frac{e^{\|S\|s_l^i h} - 1}{\|S\|} = s_l^i h$ .

Obviously, the left hand side of (33) is increasing in  $s_l^i$ , and the right hand side of (33) is decreasing in  $s_l^i$ , since  $e^{\|S\|s_l^i h}$ ,  $\gamma^{-s_l^i}$ , and  $e^{\alpha h s_l^i}$  are increasing in  $s_l^i$ . Also, when  $s_l^i = 0$ , the left hand side equals 0 and the right hand side is  $\frac{\sigma_m}{\chi_1 + \chi_3(k, h)} > 0$ . As a result, there exists a unique positive  $s(k, h)$  such that  $s_l^i > s(k, h)$ , where  $s(k, h)$  can be found by solving (28a).

The solution to (28a) is dependent on  $h$  and  $k$ , making the lower bound time-varying. To derive a time-invariant bound independent of  $k \in \mathbb{N}$ , the solution  $s(k, h) > 0$  to (28a) is discussed below based on the  $e^{\alpha h} \gamma$ .

**Case 1.**  $e^{\alpha h}\gamma < 1$ : From (28a),  $\lim_{k \rightarrow \infty} \chi_3(k, h) = \chi_2(h)$ . Then, there exists a unique time-invariant bound  $s^*$  such that  $\lim_{k \rightarrow \infty} s(k, h) = s^*(h)$ , where  $s^*(h)$  is given by (28b).

**Case 2.**  $e^{\alpha h}\gamma \geq 1$ : From (28a),  $\lim_{k \rightarrow \infty} \chi_3(k, h) = \infty$  and, therefore,  $\lim_{k \rightarrow \infty} s(k, h) = 0$  and  $\frac{e^{\|S\|sh} - 1}{\|S\|} \geq 0$ .  $\square$

If  $S = 0$  or  $S^T = -S$  implying  $\|e^{St}\| = 1$ , we further have the following corollary.

*Corollary 3:* Under Assumption 3,  $s_l^i$  has the following properties for any event-triggered mechanism in the form of (9) with the triggering function in (24):

- 1) there exists a positive  $s(k, h)$  such that

$$s_l^i > s(k, h), \quad k \in \mathbb{N}; \quad (34)$$

- 2) there exists a positive constant  $s^*$  such that

$$\lim_{k \rightarrow \infty} s(k, h) = \begin{cases} s^*(h), & e^{\alpha h}\gamma < 1, \\ 0, & e^{\alpha h}\gamma \geq 1, \end{cases} \quad (35)$$

where  $s(k, h)$  and  $s^*(h)$  are given by the following equations in  $s$  and  $s^*$ , respectively,

$$sh = \frac{\sigma_m}{\gamma^{-s}\chi_3(k, h) + \chi_1 e^{\alpha hs}},$$

$$s^*h = \frac{\sigma_m}{\gamma^{-s^*}\chi_2(h) + \chi_1 e^{\alpha hs^*}}.$$

Intuitively,  $s_l^i$  would be smaller if the bounding function  $f_i(t_k)$  decays faster than the error dynamics, that is,  $\gamma \geq e^{-\alpha h}$ , leading to more frequent event triggering. The results in Theorem 2 indicate that this may be true as  $s(k, h)$  is a decreasing function in  $k$  and lower bounded by 0, which together with  $s_l^i \in \mathbb{Z}^+$  implies that  $s_l^i \geq 1$ . By contrast, if the bounding function  $f_i(t_k)$  decays slower than the error dynamics, that is,  $\gamma < e^{-\alpha h}$ , there would be less frequent triggering as shown in (27) and (35).

Define  $\tau_l^i \triangleq s_l^i h$  as the inter-event time. Then, by following the same line as used in the proof of Theorem 2, we can establish the following result.

*Theorem 3:* Under Assumption 3,  $\tau_l^i$  has the following properties for any event-triggered mechanism in the form of (9) with the triggering function in (24):

- 1) (Time-varying bound) there exists a positive  $\tau_d(k, h)$  such that

$$\tau_l^i > \tau_d(k, h), \quad k \in \mathbb{N}; \quad (36)$$

- 2) (Asymptotic bound) there exists a positive constant  $\tau_d^*$  such that

$$\lim_{k \rightarrow \infty} \tau_d(k, h) = \begin{cases} \tau_d^*(h), & e^{\alpha h}\gamma < 1, \\ 0, & e^{\alpha h}\gamma \geq 1, \end{cases} \quad (37)$$

where  $\tau_d(k, h)$  and  $\tau_d^*(h)$  are given by the following equations in  $\tau_d$  and  $\tau_d^*$ , respectively,

$$\frac{e^{\|S\|\tau_d} - 1}{\|S\|} = \frac{\sigma_m}{\gamma^{-\frac{\tau_d}{h}}\chi_3(k, h) + \chi_1 e^{\alpha\tau_d}},$$

$$\frac{e^{\|S\|\tau_d^*} - 1}{\|S\|} = \frac{\sigma_m}{\gamma^{-\frac{\tau_d^*}{h}}\chi_2(h) + \chi_1 e^{\alpha\tau_d^*}}.$$

*Remark 2:* From the proof of Lemma 3, it is noted that  $\gamma^2 = \alpha_{i,q}\mu^2 + \beta_{i,q}\mu + \gamma_{i,q} + 1$  for some  $i \in \mathcal{V}_F$  and  $q \in \mathcal{Q}$ ,

where  $\alpha_{i,q}$ ,  $\beta_{i,q}$ , and  $\gamma_{i,q}$  are defined in (17). Based on this, it can be verified that  $\lim_{h \rightarrow 0} (\gamma^2 - 1) = 0$  and  $\lim_{h \rightarrow 0} \frac{\gamma^2 - 1}{h} = 2\text{Re}(\lambda_q) - 2\text{Re}(\lambda_i)\mu$  according to (20). Then, we have that

$$\lim_{h \rightarrow 0} (\gamma^2)^{-\frac{1}{2h}} = \lim_{h \rightarrow 0} \left[ (\gamma^2 - 1 + 1)^{\frac{1}{\gamma^2 - 1}} \right]^{-\frac{\gamma^2 - 1}{2h}} = e^{\text{Re}(\lambda_i)\mu - \text{Re}(\lambda_q)}.$$

Also,  $\lim_{h \rightarrow 0} \chi_2(h) = \chi_2^*$  for some positive  $\chi_2^*$ . As a consequence,  $\lim_{h \rightarrow 0} \tau_d^* = \tau^*$ , where  $\tau^*$  is the solution to

$$\frac{e^{\|S\|\tau^*} - 1}{\|S\|} = \frac{\sigma_m}{\chi_2^* e^{(\text{Re}(\lambda_i)\mu - \text{Re}(\lambda_q))\tau^*} + \chi_1 e^{\alpha\tau^*}}.$$

Therefore, from this and (36), it follows that, when  $h$  is sufficiently small,  $s_l^i > \tau^*/h$ . This shows that the inter-event steps and the sampling period are in a relation of almost negative proportionality, indicating that an extremely small sampling period may result in less frequent event triggering. Further analysis on the relationship between  $h$  and  $s^*(h)$  (or  $\tau_d^*(h)$ ) and related optimization will be reported elsewhere.

#### IV. COOPERATIVE OUTPUT REGULATION FOR DISTRIBUTED SYSTEMS

In order to solve Problem 1, we perform the following transformation:

$$\tilde{x}_i(t) \triangleq x_i(t) - X_i v(t) \quad \text{and} \quad \tilde{u}_i(t) \triangleq u_i(t) - U_i v(t), \quad (39)$$

where  $X_i$  and  $U_i$  are the solutions of the regulator equation in (4) for  $i \in \mathcal{V}_F$ . Then, under Assumption 2, system (2) can be written as

$$\dot{\tilde{x}}_i(t) = A_i \tilde{x}_i(t) + B_i \tilde{u}_i(t), \quad (40a)$$

$$e_i(t) = C_i \tilde{x}_i(t) + D_i \tilde{u}_i(t), \quad i \in \mathcal{V}_F. \quad (40b)$$

We first consider the distributed state feedback controller in the form of

$$u_i(t) = L_i x_i(t) - L_i X_i \eta_i(t) + U_i \eta_i(t), \quad i \in \mathcal{V}_F, \quad (41)$$

where  $L_i \in \mathbb{R}^{m_i \times n_i}$  is a matrix such that  $A_i + B_i L_i$  is Hurwitz for  $i \in \mathcal{V}_F$ , and  $\eta_i(t)$  is generated by the observer in (7). Then, we have the following result.

*Theorem 4:* Under Assumptions 1–3, Problem 1 can be solved by the distributed control law in (41).

*Proof:* From (39) and (41), we have that,

$$\begin{aligned} \tilde{u}_i(t) &= L_i x_i(t) - L_i X_i \eta_i(t) + U_i \eta_i(t) - U_i v(t) \\ &= L_i \tilde{x}_i(t) + (U_i - L_i X_i) \tilde{\eta}_i(t). \end{aligned} \quad (42)$$

Substituting (42) into equation (40) yields that

$$\dot{\tilde{x}}_i(t) = (A_i + B_i L_i) \tilde{x}_i(t) + B_i (U_i - L_i X_i) \tilde{\eta}_i(t). \quad (43)$$

As  $A_i + B_i L_i$  is Hurwitz, system (43) can be viewed as a stable system with input  $B_i (U_i - L_i X_i) \tilde{\eta}_i(t)$ . Using Theorem 1, this input converges to zero. Hence, applying Lemma 1 in [38] gives that  $\tilde{x}_i(t)$  converges to zero as  $t \rightarrow \infty$ . Finally, equation (40b) implies that  $\lim_{t \rightarrow \infty} e_i(t) = 0$ .  $\square$

Motivated by the recent work on event-triggered output regulation in [39], we further propose the following *distributed*

mixed continuous-time and periodic event-triggered state feedback controller for each follower  $i$ :

$$u_i(t) = K_i \hat{\delta}_i(t_m) + U_i \eta_i(t), \quad t \in [t_m, t_{m+1}), \quad (44)$$

where  $t_m = mT_i$ ,  $m \in \mathbb{N}$ , and  $T_i$  is the sampling period of the controller for follower  $i$ , which is non-pathological for  $(A_i, B_i)$ ;  $K_i \in \mathbb{R}^{m_i \times n_i}$ , for  $i \in \mathcal{V}_F$  is the gain matrix to be determined;  $\eta_i(t)$  is generated by the observer in (7).  $\hat{\delta}_i(t_m)$  is the event-triggered signal updated by the following event-triggered mechanism

$$\hat{\delta}_i(t_m) = \begin{cases} \delta_i(t_m) & \text{if } \|\tilde{\delta}_i(t_m)\| > g_i(t_m), \\ \hat{\delta}_i(t_m) & \text{if } \|\tilde{\delta}_i(t_m)\| \leq g_i(t_m), \end{cases} \quad (45)$$

where  $\tilde{\delta}_i(t_m) = \hat{\delta}_i(t_m) - \delta_i(\tau_m)$  and  $\delta_i(\tau_m) = x_i(t_m) - X_i \eta_i(t_m)$ ;  $g_i(t_m)$  for  $i \in \mathcal{V}_F$  is a positive bounded function and converges to zero as  $t_m \rightarrow \infty$ . Obviously,  $\hat{\delta}_i(t_m)$  is a subsequence of the sampled states  $\delta_i(t_m)$ . From (39) and (44), we have that,  $\forall t \in [t_m, t_{m+1})$ ,

$$\begin{aligned} \tilde{u}_i(t) &= K_i \hat{\delta}_i(t_m) + U_i \eta_i(t) - U_i v(t) \\ &= K_i [\tilde{x}_i(t_m) + \tilde{\delta}_i(t_m) - X_i \tilde{\eta}_i(t_m)] + U_i \tilde{\eta}_i(t). \end{aligned} \quad (46)$$

Substituting (46) into equation (40) gives that

$$\begin{aligned} \dot{\tilde{x}}_i(t) &= A_i \tilde{x}_i(t) + B_i K_i [\tilde{x}_i(t_m) + \tilde{\delta}_i(t_m)] \\ &\quad - B_i K_i X_i \tilde{\eta}_i(t_m) + B_i U_i \tilde{\eta}_i(t). \end{aligned} \quad (47)$$

Let  $A_{di} = e^{A_i T_i}$  and  $B_{di} = \int_0^{T_i} e^{A_i \tau} d\tau B_i$ . Then,

$$\begin{aligned} \tilde{x}_i(t_{m+1}) &= (A_{di} + B_{di} K_i) \tilde{x}_i(t_m) + \Delta_i(t_m) \\ &\quad + B_{di} K_i [\tilde{\delta}_i(t_m) - X_i \tilde{\eta}_i(t_m)], \end{aligned} \quad (48)$$

where  $\Delta_i(t_m) = \int_0^{T_i} e^{A_i(T_i-\tau)} B_i U_i \tilde{\eta}_i(t_m + \tau) d\tau$ . From Theorem 3.2 in [12], we can always select a  $K_i$  such that  $A_{di} + B_{di} K_i$  is Schur for  $i \in \mathcal{V}_F$ . Then, we have the following result.

*Theorem 5:* Under Assumptions 1–3, Problem 1 can be solved by the distributed control law in (44).

*Proof:* Obviously, we have that

$$\|\Delta_i(t_m)\| \leq T_i e^{\|A_i\| T_i} \|B_i U_i\| \max_{\tau \in [t_m, t_{m+1})} \|\tilde{\eta}_i(\tau)\|. \quad (49)$$

From Theorem 1, it follows that  $\lim_{\tau \rightarrow \infty} \tilde{\eta}_i(\tau) = 0$ , which implies  $\lim_{t_m \rightarrow \infty} \Delta_i(t_m) = 0$ . The event-triggered mechanism (45) enforces  $\|\tilde{\delta}_i(t_m)\| \leq g_i(t_m)$  after the updating, and thus  $\lim_{t_m \rightarrow \infty} \tilde{\delta}_i(t_m) = 0$ . Hence, system (48) is a stable system with the input  $\Delta_i(t_m) + B_{di} K_i [\tilde{\delta}_i(t_m) - X_i \tilde{\eta}_i(t_m)]$ , which converges to zero. Applying Lemma 2 to system (48) yields that  $\lim_{t_m \rightarrow \infty} \tilde{x}_i(t_m) = 0$ . Then, it follows from system (45) and the solution to (47) that, for  $t \in [t_m, t_{m+1})$ ,

$$\begin{aligned} \|\tilde{x}_i(t)\| &\leq \left[ 1 + T_i \|B_i K_i\| \right] \|\tilde{x}_i(t_m)\| e^{\|A_i\| T_i} \\ &\quad + T_i e^{\|A_i\| T_i} \|B_i\| [g_i(t_m) + \|X_i\| \|\tilde{\eta}_i(t_m)\|] \\ &\quad + T_i e^{\|A_i\| T_i} \|B_i U_i\| \max_{\tau \in [t_m, t_{m+1})} \|\tilde{\eta}_i(\tau)\|. \end{aligned}$$

For any monotonically increasing sequence  $\{t_m\}_{m \in \mathbb{N}}$  such that  $t_m \rightarrow \infty$  as  $m \rightarrow \infty$ , we have that  $\lim_{m \rightarrow \infty} \tilde{x}_i(t_m) = 0$ ,

$\lim_{t_m \rightarrow \infty} \tilde{\eta}_{M_i}(t_m) = 0$ ,  $\lim_{t_m \rightarrow \infty} \tilde{\eta}_i(t_m) = 0$ , and  $\lim_{t_m \rightarrow \infty} g_i(t_m) = 0$ . Therefore,  $\lim_{t \rightarrow \infty} \tilde{x}_i(t) = 0$ . Finally, equation (40b) implies that  $\lim_{t \rightarrow \infty} e_i(t) = 0$ .  $\square$

## V. NUMERICAL EXAMPLES

### A. Example 1: Time-triggered observers



Figure 2. Communication topology  $\mathcal{G}$

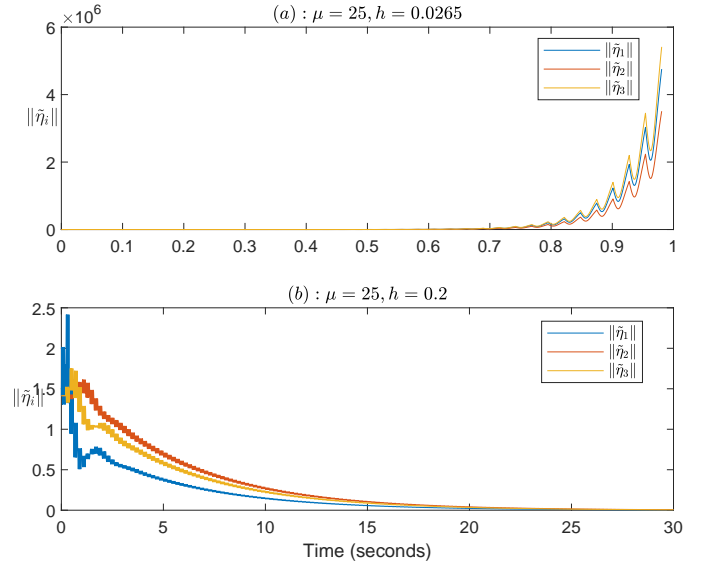


Figure 3. Estimation errors with different parameters

Consider a distributed systems shown in Figure 2 with

$$S = \begin{bmatrix} 0 & 100 \\ -100 & 0 \end{bmatrix} \quad \text{and} \quad H = \begin{bmatrix} 2 & -1 & 0 \\ 0 & 1 & -1 \\ -1 & -1 & 2 \end{bmatrix}.$$

The eigenvalues of  $H$  are  $\{2.4196 \pm 0.6063i, 0.1067\}$ , implying  $\theta_i \in \{0, \pm 0.2455\}$ .

It can be easily verified that  $h = 0.0265$  is a pathological sampling period over the graph, and thus  $\mu$  does not exist for this sampling period. The simulation in Figure 3.(a) shows that the estimation errors don't converge to 0 as we analyzed.

$h = 0.2$  is a non-pathological sampling period according to Corollary 2, and the corresponding feasible interval of  $\mu$  is  $\bigcap_{q \in \{1,2\}, i \in \{1,2,3\}} (\underline{\mu}_{i,q}, \bar{\mu}_{i,q}) = (0, 50.2333)$ . We choose  $\mu = 25$  and the estimation errors converge to 0 as depicted in Figure 3.(b). This simple example shows that even a small sampling period may not guarantee the convergence due to the existence of pathological sampling periods.

### B. Example 2: Mixed time- and event-triggered observers

In this example, we consider a linear distributed system composed of one leader and four followers in the form of

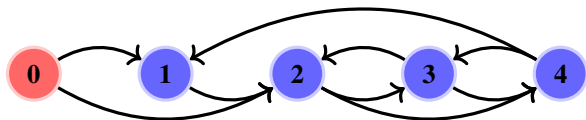


Figure 4. Communication topology  $\mathcal{G}$

(1) with  $S = \begin{bmatrix} 0 & 1 \\ -1 & 0 \end{bmatrix}$ . It can be easily calculated  $\|e^{St}\| = 1$ .  $v(t) \in \mathbb{R}^2$  can be measured by followers 1 and 2 as shown in Figure 4. The matrix  $H$  for this example can be determined as

$$H = \begin{bmatrix} 2 & 0 & 0 & -1 \\ -1 & 3 & -1 & 0 \\ 0 & -1 & 2 & -1 \\ 0 & -1 & -1 & 2 \end{bmatrix}.$$

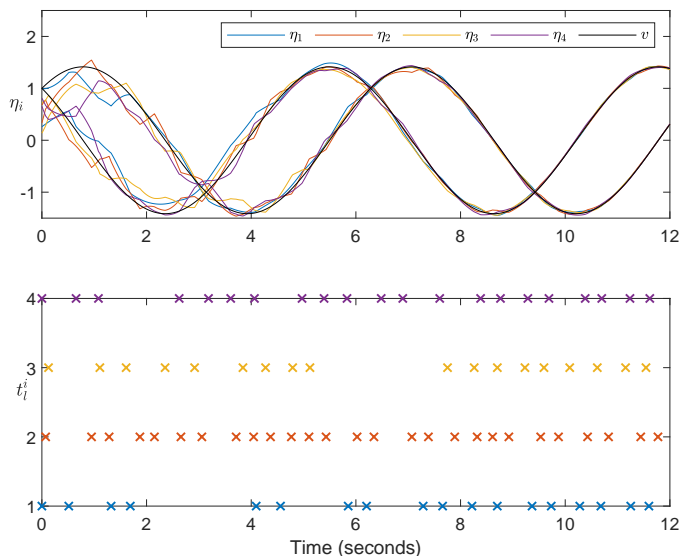


Figure 5. Estimation performance of all followers.

We design a mixed time- and event-triggered distributed observers composed of (7) with the event-triggered condition in (9) where  $f_i(t_k) = \sigma_i e^{-\alpha_i t_k}$ . Simulations are conducted with the following parameters:  $\mu = 1.5$ ,  $\sigma_i = 1$  and  $h = 0.001$ . It can be verified that  $\gamma = 0.9994$  and  $\beta = 1.0004$ . Figure 5 shows the estimation performance of all followers with  $\alpha = 0.25$ . The inter-event steps  $s_i^j$  and  $s(k, h)$  for the case  $\gamma e^{\alpha h} < 1$  with  $\alpha = 0.25$  and for the case  $\gamma e^{\alpha h} \geq 1$  with  $\alpha = 2$  are shown in Figure 6.(a) and Figure 6.(b), respectively. It can be seen from the figure that slow triggering functions ( $\gamma e^{\alpha h} < 1$ ) will probably increase the inter-event steps  $s_i^j$ , and fast triggering function ( $\gamma e^{\alpha h} \geq 1$ ) may lead to the degradation of event-triggered system to a pure sampled-data system.

### C. Example 3: Multiple mobile robots

Consider a group of mobile robots described by multiple double integrators [40]:

$$\dot{x}_{hi}(t) = v_{xi}(t), \quad \dot{v}_{xi}(t) = \bar{u}_{xi}(t),$$

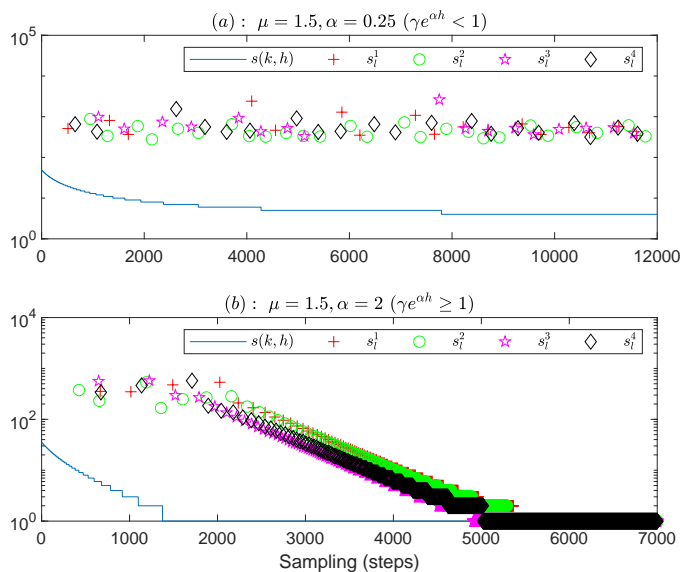


Figure 6. Inter-event steps.

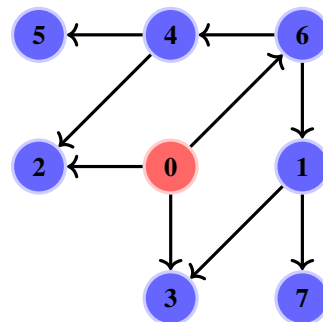


Figure 7. Communication topology  $\mathcal{G}$  and desired formation pattern

$$\dot{y}_{hi}(t) = v_{yi}(t), \quad \dot{v}_{yi}(t) = \bar{u}_{yi}(t), \quad (50)$$

where  $v_{xi}(t) \in \mathbb{R}$  and  $v_{yi}(t) \in \mathbb{R}$  represent the velocity along the  $X$  and  $Y$  axis, respectively. For  $i \in \mathcal{V}_F$ ,  $h_i(t) = \text{col}(x_{hi}(t), y_{hi}(t))$  represents the position of the  $i$ th mobile robot.

We consider the leader-following formation control problem where the leader and followers move in a formation pattern shown in Figure 7 with a constant speed. Thus, the control objective is to find a distributed control input such that

$$\lim_{t \rightarrow \infty} (h_i(t) - h_0(t)) = h_{di} \quad \text{and} \quad \lim_{t \rightarrow \infty} (\dot{h}_i(t) - \dot{h}_0(t)) = 0,$$

where  $h_0(t) = \text{col}(v_x t + p_x, v_y t + p_y)$  is the reference input, and  $h_{di} = \text{col}(x_{di}, y_{di})$  is the relative position between the  $i$ th follower and the leader, for  $i = 1, \dots, 7$ . The regulated errors are defined as:

$$e_i(t) = (h_i(t) - h_{di}) - h_0(t), \quad i = 1, \dots, 7.$$

The reference input  $h_0(t) = ([1 \ 0] \otimes I_2)v(t)$  can be generated by system (1) with the following initial condition and system matrix

$$v(0) = \text{col}(v_x, v_y, p_x, p_y) \quad \text{and} \quad S = \begin{bmatrix} 0 & 1 \\ 0 & 0 \end{bmatrix} \otimes I_2.$$

The system composed of (50) and  $e_i$  has the form (2) with the state

$$x_i(t) = \text{col}(x_{hi}(t) - x_{di}, y_{hi}(t) - y_{di}, v_{xi}(t), v_{yi}(t)),$$

output  $e_i$ , input  $u_i$ , and various matrices

$$A_i = \begin{bmatrix} 0 & 1 \\ 0 & 0 \end{bmatrix} \otimes I_2, \quad B_i = \begin{bmatrix} 0 \\ 1 \end{bmatrix} \otimes I_2, \quad P_i = 0_{4 \times 4},$$

$$C_i = \begin{bmatrix} 1 & 0 \end{bmatrix} \otimes I_2, \quad D_i = 0_{2 \times 4}, \quad F_i = \begin{bmatrix} -1 & 0 \end{bmatrix} \otimes I_2.$$

Then, the solution to (4) is  $(X_i, U_i) = (I_4, 0_{2 \times 4})$ .

We now design a mixed time- and event-triggered distributed controller composed of (7) and (44) with the event-triggered condition in (9) and (45) where  $f_i(t_k) = \sigma_i e^{-\alpha_i t_k}$  and  $g_i(t_m) = \gamma_i \log(1 + e^{-\beta_i t_m})$ , respectively. The parameters are given as follows:  $h_{d1} = \text{col}(0, 20)$ ,  $h_{d2} = \text{col}(0, -20)$ ,  $h_{d3} = \text{col}(-20, 0)$ ,  $h_{d4} = \text{col}(20, 0)$ ,  $h_{d5} = \text{col}(20, -20)$ ,  $h_{d6} = \text{col}(20, 20)$ ,  $h_{d7} = \text{col}(20, 20)$ ,  $\sigma_i = 30$ ,  $\alpha_i = 0.8$ ,  $\gamma_i = 35$ ,  $\beta_i = 0.4$ ,  $K_{1i} = [-4, -2] \otimes I_2$ ,  $\mu = 10$ ,  $h = 0.01$ ,  $T_i = 0.05$ , for  $i = 1, \dots, 7$ . It can be verified that Assumptions 1 to 3 are all satisfied. Simulations are conducted with following initial conditions:

$$x_1(0) = \text{col}(-5, 18, 0, 0), \quad x_2(0) = \text{col}(3, -14, 0, 0),$$

$$x_3(0) = \text{col}(-2, -9, 0, 0), \quad x_4(0) = \text{col}(0, 5, 0, 0),$$

$$x_5(0) = \text{col}(9, 4, 0, 0), \quad x_6(0) = \text{col}(21, 26, 0, 0),$$

$$x_7(0) = \text{col}(-16, -9, 0, 0), \quad v(0) = \text{col}(11, 11, 5, 5),$$

$$\eta_i(0) = 0, \quad \hat{\eta}_i(0) = 0, \quad i = 1, \dots, 7.$$

Figure 8 shows the trajectories of the seven robots and the

**Figure 8.** Animation( open with Adobe): Formation performance.

leader. Figure 9 shows the estimation error trajectories of  $\|\hat{\eta}_i\|$ , which all converge to zero. Figure 10 shows the regulated error trajectories of  $\|e_i\|$ , which all converge to zero as well.

## VI. CONCLUSIONS

In this paper, the problem of cooperative output regulation for heterogeneous linear distributed systems has been investigated by using mixed time- and event-triggered observers. A

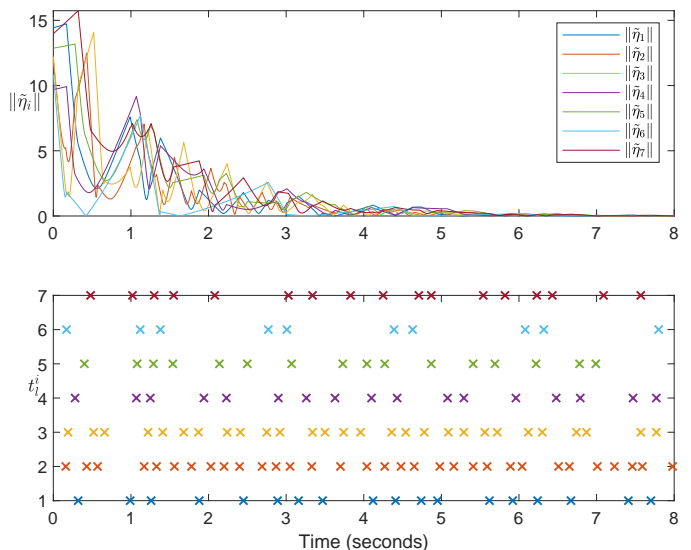


**Figure 9.** Estimation errors of all followers,  $i = 1, \dots, 7$ .

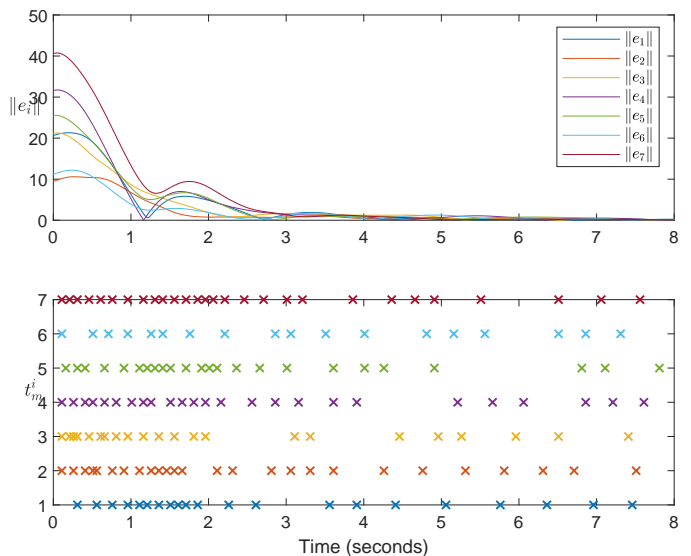


**Figure 10.** Tracking errors of all followers,  $i = 1, \dots, 7$ .

distributed observer with time-triggered observations has been proposed to reconstruct the state of the leader, and an auxiliary observer with event-triggered communication has been designed to reduce the information exchange among followers. Event triggering is based on local sampled information and local computation, and Zeno behavior is naturally excluded. All feasible sampling periods for the observability of the connected systems have been given, revealing some fundamental relationships among sampling periods, topologies, and system dynamics in distributed systems. Time-varying and asymptotic bounds for the inter-event steps and time have been given, and their relationship with periodic sampling and event triggering has been shown. Utilizing the estimation state of the leader, two distributed control laws have been synthesized to solve the cooperative output regulation problem. Three numerical examples have been provided to show the effectiveness of the proposed control approach.

## APPENDIX A

(1) Construct an auxiliary function

$$f(x, y) = e^{2xh} - 2e^{xh} \cos(yh) + 1,$$

where  $x, y \in \mathbb{R}$ . Taking Taylor series expansion around the origin yields that

$$\begin{aligned} f(x, y) &= f(0, 0) + x \frac{\partial f}{\partial x}(0, 0) + y \frac{\partial f}{\partial y}(0, 0) + \frac{1}{2} [x^2 \frac{\partial^2 f}{\partial x^2}(0, 0) \\ &\quad + 2xy \frac{\partial^2 f}{\partial x \partial y}(0, 0) + y^2 \frac{\partial^2 f}{\partial y^2}(0, 0)] + o(\rho^2) \\ &= \rho^2 h^2 + o(\rho^2), \end{aligned}$$

where  $\rho = \sqrt{x^2 + y^2}$ , and  $o(\rho^2)$  is the Peano remainder such that  $\lim_{\rho \rightarrow 0} \frac{o(\rho^2)}{\rho^2} = 0$ . Noting that  $V_q^2(h) + U_q^2(h) = f(\operatorname{Re}(\lambda_q), \operatorname{Im}(\lambda_q))$ , we have that

$$\begin{aligned} \frac{V_q^2(h) + U_q^2(h)}{|\lambda_q|^2} &= \frac{h^2 |\lambda_q|^2 + o(|\lambda_q|^2)}{|\lambda_q|^2} \\ &= h^2 + \frac{o(|\lambda_q|^2)}{|\lambda_q|^2}. \end{aligned}$$

Hence,

$$\lim_{\lambda_q \rightarrow 0} \frac{V_q^2(h) + U_q^2(h)}{|\lambda_q|^2} = h^2. \quad (\text{A.1})$$

(2) Construct two auxiliary functions

$$\begin{aligned} g(x, y) &= \sin(yh)x - e^{xh}y + \cos(yh)y, \\ p(x, y) &= \sin(yh)y + e^{xh}x - \cos(yh)x, \end{aligned}$$

where  $x, y \in \mathbb{R}$ . Taking Taylor series expansion around the origin yields that

$$\begin{aligned} g(x, y) &= g(0, 0) + x \frac{\partial g}{\partial x}(0, 0) + y \frac{\partial g}{\partial y}(0, 0) + \frac{1}{2} [x^2 \frac{\partial^2 g}{\partial x^2}(0, 0) \\ &\quad + 2xy \frac{\partial^2 g}{\partial x \partial y}(0, 0) + y^2 \frac{\partial^2 g}{\partial y^2}(0, 0)] + o(\rho^2) \\ &= o(\rho^2), \end{aligned}$$

$$\begin{aligned} p(x, y) &= p(0, 0) + x \frac{\partial p}{\partial x}(0, 0) + y \frac{\partial p}{\partial y}(0, 0) + \frac{1}{2} [x^2 \frac{\partial^2 p}{\partial x^2}(0, 0) \\ &\quad + 2xy \frac{\partial^2 p}{\partial x \partial y}(0, 0) + y^2 \frac{\partial^2 p}{\partial y^2}(0, 0)] + o(\rho^2) \\ &= h\rho^2 + o(\rho^2), \end{aligned}$$

where  $\rho = \sqrt{x^2 + y^2}$ , and  $o(\rho^2)$  is the Peano remainder such that  $\lim_{\rho \rightarrow 0} \frac{o(\rho^2)}{\rho^2} = 0$ . Since

$$\begin{aligned} V_q(h)\operatorname{Re}(\lambda_q) - U_q(h)\operatorname{Im}(\lambda_q) &= g(\operatorname{Re}(\lambda_q), \operatorname{Im}(\lambda_q)), \\ U_q(h)\operatorname{Re}(\lambda_q) + V_q(h)\operatorname{Im}(\lambda_q) &= p(\operatorname{Re}(\lambda_q), \operatorname{Im}(\lambda_q)), \end{aligned}$$

we have that

$$\begin{aligned} \frac{V_q(h)\operatorname{Re}(\lambda_q) - U_q(h)\operatorname{Im}(\lambda_q)}{|\lambda_q|^2} &= \frac{o(|\lambda_q|^2)}{|\lambda_q|^2}, \\ \frac{U_q(h)\operatorname{Re}(\lambda_q) + V_q(h)\operatorname{Im}(\lambda_q)}{|\lambda_q|^2} &= h + \frac{o(|\lambda_q|^2)}{|\lambda_q|^2}. \end{aligned}$$

Hence,

$$\begin{aligned} \lim_{\lambda_q \rightarrow 0} \frac{V_q(h)\operatorname{Re}(\lambda_q) - U_q(h)\operatorname{Im}(\lambda_q)}{|\lambda_q|^2} &= 0, \\ \lim_{\lambda_q \rightarrow 0} \frac{U_q(h)\operatorname{Re}(\lambda_q) + V_q(h)\operatorname{Im}(\lambda_q)}{|\lambda_q|^2} &= h. \end{aligned} \quad (\text{A.2})$$

Next, we will prove that **(a)**  $(\phi_q(h) - \theta_q) \in (-\pi, \pi)$  when  $\lambda_q \rightarrow 0$ ; **(b)**  $\lim_{\lambda_q \rightarrow 0} \sin(\phi_q(h) - \theta_q) = 0$ ; **(c)**  $\lim_{\lambda_q \rightarrow 0} \cos(\phi_q(h) - \theta_q) = 1$ .

**(a)** We discuss the following three cases based on  $\lambda_q$ :

**Case i.**  $\operatorname{Re}(\lambda_q) = 0$  and  $\operatorname{Im}(\lambda_q) \neq 0$ : On one hand, as  $\operatorname{Re}(\lambda_q) = 0$ ,  $\lim_{\operatorname{Im}(\lambda_q) \rightarrow 0^+} \theta_q = \frac{\pi}{2}$  or  $\lim_{\operatorname{Im}(\lambda_q) \rightarrow 0^-} \theta_q = -\frac{\pi}{2}$ . On the other hand, when  $\operatorname{Re}(\lambda_q) = 0$ ,  $\phi_q(h) = \operatorname{Arg}((1 - \cos(\operatorname{Im}(\lambda_q)h) + \sin(\operatorname{Im}(\lambda_q)h))j)$ , which implies that

$$\lim_{\operatorname{Im}(\lambda_q) \rightarrow 0^+} \phi_q(h) = \frac{\pi}{2} \quad \text{or} \quad \lim_{\operatorname{Im}(\lambda_q) \rightarrow 0^-} \phi_q(h) = -\frac{\pi}{2}.$$

**Case ii.**  $\operatorname{Re}(\lambda_q) \neq 0$  and  $\operatorname{Im}(\lambda_q) = 0$ : Since  $\operatorname{Im}(\lambda_q) = 0$  and  $\operatorname{Re}(\lambda_q) \neq 0$ ,  $\theta_q = 0$  and  $\phi_q(h) = \operatorname{Arg}((e^{\operatorname{Re}(\lambda_q)h} - 1) + 0j) = 0$ .

**Case iii.**  $\operatorname{Re}(\lambda_q) \neq 0$  and  $\operatorname{Im}(\lambda_q) \neq 0$ : when  $\operatorname{Im}(\lambda_q) \rightarrow 0$ ,  $\sin(\operatorname{Im}(\lambda_q)h)$  and  $\operatorname{Im}(\lambda_q)$  have the same sign. Hence,  $\theta_q = \operatorname{Arg}(\operatorname{Re}(\lambda_q) + \operatorname{Im}(\lambda_q)j)$  and  $\phi_q(h) = \operatorname{Arg}((e^{\operatorname{Re}(\lambda_q)h} - \cos(\operatorname{Im}(\lambda_q)h)) + \sin(\operatorname{Im}(\lambda_q)h)j)$  are either in the first/second quadrant or in the third/fourth quadrant at the same time.

Combining Cases i to iii gives that  $(\phi_q(h) - \theta_q) \in (-\pi, \pi)$  when  $\lambda_q \rightarrow 0$ .

**(b)** Applying the angle difference identity of the sine function yields that

$$\begin{aligned} \sin(\phi_q(h) - \theta_q) &= \sin(\phi_q(h)) \cos(\theta_q) - \cos(\phi_q(h)) \sin(\theta_q) \\ &= \frac{V_q(h)\operatorname{Re}(\lambda_q)}{|\lambda_q| \sqrt{V_q^2(h) + U_q^2(h)}} - \frac{U_q(h)\operatorname{Im}(\lambda_q)}{|\lambda_q| \sqrt{V_q^2(h) + U_q^2(h)}} \\ &= \frac{V_q(h)\operatorname{Re}(\lambda_q) - U_q(h)\operatorname{Im}(\lambda_q)}{|\lambda_q|^2} \frac{|\lambda_q|}{\sqrt{V_q^2(h) + U_q^2(h)}}. \end{aligned}$$

From (A.1) and (A.2), it follows that  $\lim_{\lambda_q \rightarrow 0} \sin(\phi_q(h) - \theta_q) = 0$ .

**(c)** Applying the angle difference identity of the cosine function yields that

$$\begin{aligned} \cos(\phi_q(h) - \theta_q) &= \cos(\phi_q(h)) \cos(\theta_q) + \sin(\phi_q(h)) \sin(\theta_q) \\ &= \frac{U_q(h)\operatorname{Re}(\lambda_q)}{|\lambda_q| \sqrt{V_q^2(h) + U_q^2(h)}} + \frac{V_q(h)\operatorname{Im}(\lambda_q)}{|\lambda_q| \sqrt{V_q^2(h) + U_q^2(h)}} \\ &= \frac{U_q(h)\operatorname{Re}(\lambda_q) + V_q(h)\operatorname{Im}(\lambda_q)}{|\lambda_q|^2} \frac{|\lambda_q|}{\sqrt{V_q^2(h) + U_q^2(h)}}. \end{aligned}$$

From (A.1) and (A.2), it follows that  $\lim_{\lambda_q \rightarrow 0} \cos(\phi_q(h) - \theta_q) = 1$ .

By (a) and the continuity of the sine and cosine functions, there is only one limit point of  $\phi_q(h) - \theta_q$ , that is, 0, in the closure of  $(-\pi, \pi)$  such that (b) and (c) hold. Therefore,  $\lim_{\lambda_q \rightarrow 0} (\phi_q(h) - \theta_q) = 0$ .

**(3)** It is easy to verify that

$$\begin{aligned} \lim_{h \rightarrow 0} U_q(h) &= 0, \\ \lim_{h \rightarrow 0} V_q(h) &= 0, \\ \dot{U}_q(h) &= \operatorname{Re}(\lambda_q) e^{\operatorname{Re}(\lambda_q)h} + \operatorname{Im}(\lambda_q) \sin(\operatorname{Im}(\lambda_q)h), \\ \dot{V}_q(h) &= \operatorname{Im}(\lambda_q) \cos(\operatorname{Im}(\lambda_q)h). \end{aligned}$$

Then, by using the L'Hôpital's rule and these equalities, we have that

$$\begin{aligned}
& \lim_{h \rightarrow 0} \frac{U_q^2(h) + V_q^2(h)}{h^2} \\
&= \lim_{h \rightarrow 0} \frac{U_q(h) \dot{U}_q(h) + V_q(h) \dot{V}_q(h)}{h} \\
&= \lim_{h \rightarrow 0} \left[ U_q(h) \ddot{U}_q(h) + \dot{U}_q^2(h) + V_q(h) \ddot{V}_q(h) + \dot{V}_q^2(h) \right] \\
&= \lim_{h \rightarrow 0} \left[ \dot{U}_q^2(h) + \dot{V}_q^2(h) \right] = |\lambda_q|^2
\end{aligned}$$

(4) By following the same line as used in the proof of (a), we have that  $(\phi_q(h) - \theta_q) \in (-\pi, \pi)$  when  $h \rightarrow 0$ . Then, using L'Hôpital's rule gives that

$$\begin{aligned}
\lim_{h \rightarrow 0} \frac{V_q(h)}{U_q(h)} &= \lim_{h \rightarrow 0} \frac{\sin(\text{Im}(\lambda_q)h)}{e^{\text{Re}(\lambda_q)h} - \cos(\text{Im}(\lambda_q)h)} \\
&= \lim_{h \rightarrow 0} \frac{\text{Im}(\lambda_q) \cos(\text{Im}(\lambda_q)h)}{\text{Re}(\lambda_q)e^{\text{Re}(\lambda_q)h} + \text{Im}(\lambda_q) \sin(\text{Im}(\lambda_q)h)} \\
&= \frac{\text{Im}(\lambda_q)}{\text{Re}(\lambda_q)} = \tan(\theta_q),
\end{aligned}$$

which together with  $(\phi_q(h) - \theta_q) \in (-\pi, \pi)$  implies that

$$\lim_{h \rightarrow 0} (\phi_q(h) - \theta_q) = 0.$$

#### APPENDIX B

$\alpha_{i,q}$ ,  $\beta_{i,q}$ , and  $\gamma_{i,q}$  are evaluated as follows:

$$\begin{aligned}
\alpha_{i,q} &= \frac{|\lambda_i|^2}{|\lambda_q|^2} |e^{\lambda_q h} - 1|^2 \\
&= \frac{|\lambda_i|^2}{|\lambda_q|^2} \left( e^{2\text{Re}(\lambda_q)h} - 2e^{\text{Re}(\lambda_q)h} \cos(\text{Im}(\lambda_q)h) + 1 \right) \\
&= \frac{|\lambda_i|^2}{|\lambda_q|^2} (V_q^2(h) + U_q^2(h)), \\
\beta_{i,q} &= - \int_0^h [\lambda_i e^{\lambda_q \tau + \lambda_q^* h} + \lambda_i^* e^{\lambda_q^* \tau + \lambda_q h}] d\tau \\
&= |\lambda_i| \int_0^h [e^{\theta_i j} e^{\lambda_q \tau + \lambda_q^* h} + e^{-\theta_i j} e^{\lambda_q^* \tau + \lambda_q h}] d\tau \\
&= - \frac{|\lambda_i|}{|\lambda_q|^2} [\lambda_q^* e^{\lambda_q h + \lambda_q^* h + \theta_i j} + \lambda_q e^{\lambda_q^* h + \lambda_q h - \theta_i j} \\
&\quad - \lambda_q^* e^{\lambda_q^* h + \theta_i j} - \lambda_q e^{\lambda_q h - \theta_i j}] \\
&= - \frac{|\lambda_i|}{|\lambda_q|} [e^{\lambda_q h + \lambda_q^* h + \theta_i j - \theta_q j} - e^{\lambda_q^* h + \theta_i j - \theta_q j} \\
&\quad + e^{\lambda_q^* h + \lambda_q h - \theta_i j + \theta_q j} - e^{\lambda_q h - \theta_i j + \theta_q j}] \\
&= - 2 \frac{|\lambda_i|}{|\lambda_q|} e^{\text{Re}(\lambda_q)h} [\cos(\theta_i - \theta_q) e^{\text{Re}(\lambda_q)h} \\
&\quad - \cos(\text{Im}(\lambda_q)h - \theta_i + \theta_q)] \\
&= - 2 \frac{|\lambda_i|}{|\lambda_q|} e^{\text{Re}(\lambda_q)h} [\cos(\theta_i - \theta_q) U_q(h) \\
&\quad - V_q(h) \sin(\theta_i - \theta_q)] \\
&= - 2 \frac{|\lambda_i|}{|\lambda_q|} e^{\text{Re}(\lambda_q)h} \sqrt{V_q^2(h) + U_q^2(h)} \cos(\psi_{i,q}(h)), \\
\gamma_{i,q} &= e^{2\text{Re}(\lambda_q)h} - 1,
\end{aligned}$$

where  $\psi_{i,q}(h)$ ,  $U_q(h)$ , and  $V_q(h)$  are defined in (6). Then, we have that

$$\begin{aligned}
& \beta_{i,q}^2 - 4\alpha_{i,q}\gamma_{i,q} \\
&= 4 \frac{|\lambda_i|^2}{|\lambda_q|^2} e^{2\text{Re}(\lambda_q)h} (V_q^2(h) + U_q^2(h)) \cos^2(\psi_{i,q}(h)) \\
&\quad - 4 \frac{|\lambda_i|^2}{|\lambda_q|^2} (V_q^2(h) + U_q^2(h)) (e^{2\text{Re}(\lambda_q)h} - 1) \\
&= 4 \frac{|\lambda_i|^2}{|\lambda_q|^2} (V_q^2(h) + U_q^2(h)) [1 - e^{2\text{Re}(\lambda_q)h} \sin^2(\psi_{i,q}(h))].
\end{aligned}$$

#### REFERENCES

- [1] A. V. Proskurnikov and M. Cao, "Synchronization of pulse-coupled oscillators and clocks under minimal connectivity assumptions," *IEEE Transactions on Automatic Control*, vol. 62, no. 11, pp. 5873–5879, 2016.
- [2] J. I. Poveda and A. R. Teel, "Hybrid mechanisms for robust synchronization and coordination of multi-agent networked sampled-data systems," *Automatica*, vol. 99, pp. 41–53, 2019.
- [3] W. Ren and R. W. Beard, "Consensus seeking in multi-agent systems under dynamically changing interaction topologies," *IEEE Transactions on Automatic Control*, vol. 50, no. 5, pp. 655–661, 2005.
- [4] F. D. Prisco, A. Isidori, L. Marconi, and A. Pietrabissa, "Leader-following coordination of nonlinear agents under time-varying communication topologies," *IEEE Transactions on Control of Network Systems*, vol. 2, no. 4, pp. 393–405, 2015.
- [5] R. Vidal, O. Shakhmurov, and S. Sastry, "Formation control of nonholonomic mobile robots with omnidirectional visual servoing and motion segmentation," in *2003 IEEE International Conference on Robotics and Automation (Cat. No. 03CH37422)*, vol. 1. IEEE, 2003, pp. 584–589.
- [6] S. Mou, M. Cao, and A. S. Morse, "Target-point formation control," *Automatica*, vol. 61, pp. 113–118, 2015.
- [7] X. Li, Y. C. Soh, L. Xie, and F. L. Lewis, "Cooperative output regulation of heterogeneous linear multi-agent networks via  $H_\infty$  performance allocation," *IEEE Transactions on Automatic Control*, vol. 64, no. 2, pp. 683–696, 2018.
- [8] Y. Su and J. Huang, "Cooperative output regulation of linear multi-agent systems," *IEEE Transactions on Automatic Control*, vol. 57, no. 4, pp. 1062–1066, 2011.
- [9] A. Isidori, L. Marconi, and G. Casadei, "Robust output synchronization of a network of heterogeneous nonlinear agents via nonlinear regulation theory," *IEEE Transactions on Automatic Control*, vol. 59, no. 10, pp. 2680–2691, 2014.
- [10] J. Xiang, Y. Li, and D. J. Hill, "Cooperative output regulation of linear multi-agent network systems with dynamic edges," *Automatica*, vol. 77, pp. 1–13, 2017.
- [11] J. Huang, "Certainty equivalence, separation principle, and cooperative output regulation of multiagent systems by the distributed observer approach," in *Control of Complex Systems*. Elsevier, 2016, pp. 421–449.

- [12] T. Chen and B. A. Francis, *Optimal sampled-data control systems*. London U.K.: Springer Science & Business Media, 1995.
- [13] —, “ $H_2$ -optimal sampled-data control,” *IEEE Transactions on Automatic Control*, vol. 36, no. 4, pp. 387–397, 1991.
- [14] K. J. Astrom and B. M. Bernhardsson, “Comparison of Riemann and Lebesgue sampling for first order stochastic systems,” in *Proceedings of the 41st IEEE Conference on Decision and Control, 2002.*, vol. 2. IEEE, 2002, pp. 2011–2016.
- [15] X. Meng and T. Chen, “Optimal sampling and performance comparison of periodic and event based impulse control,” *IEEE Transactions on Automatic Control*, vol. 57, no. 12, pp. 3252–3259, 2012.
- [16] D. P. Borgers and W. M. H. Heemels, “Event-separation properties of event-triggered control systems,” *IEEE Transactions on Automatic Control*, vol. 59, no. 10, pp. 2644–2656, 2014.
- [17] H. Yu and T. Chen, “On zeno behavior in event-triggered finite-time consensus of multi-agent systems,” *IEEE Transactions on Automatic Control*.
- [18] W. Liu and J. Huang, “Event-triggered cooperative robust practical output regulation for a class of linear multi-agent systems,” *Automatica*, vol. 85, pp. 158–164, 2017.
- [19] W. Hu, L. Liu, and G. Feng, “Cooperative output regulation of linear multi-agent systems by intermittent communication: A unified framework of time- and event-triggering strategies,” *IEEE Transactions on Automatic Control*, vol. 63, no. 2, pp. 548–555, 2017.
- [20] —, “Event-triggered cooperative output regulation of linear multi-agent systems under jointly connected topologies,” *IEEE Transactions on Automatic Control*, vol. 64, no. 3, pp. 1317–1322, 2018.
- [21] W. Liu and J. Huang, “Cooperative global robust output regulation for a class of nonlinear multi-agent systems by distributed event-triggered control,” *Automatica*, vol. 93, pp. 138–148, 2018.
- [22] X. Meng and T. Chen, “Event based agreement protocols for multi-agent networks,” *Automatica*, vol. 49, no. 7, pp. 2125–2132, 2013.
- [23] T. Liu, M. Cao, C. De Persis, and J. M. Hendrickx, “Distributed event-triggered control for asymptotic synchronization of dynamical networks,” *Automatica*, vol. 86, pp. 199–204, 2017.
- [24] T.-H. Cheng, Z. Kan, J. R. Klotz, J. M. Shea, and W. E. Dixon, “Event-triggered control of multiagent systems for fixed and time-varying network topologies,” *IEEE Transactions on Automatic Control*, vol. 62, no. 10, pp. 5365–5371, 2017.
- [25] Y. Y. Qian, L. Liu, and G. Feng, “Cooperative output regulation of linear multi-agent systems: An event-triggered adaptive distributed observer approach,” *IEEE Transactions on Automatic Control*, vol. 66, no. 2, pp. 833–840, 2021.
- [26] X. Meng, L. Xie, and Y. C. Soh, “Event-triggered output regulation of heterogeneous multiagent networks,” *IEEE Transactions on Automatic Control*, vol. 63, no. 12, pp. 4429–4434, 2018.
- [27] B. Cheng and Z. Li, “Coordinated tracking control with asynchronous edge-based event-triggered communications,” *IEEE Transactions on Automatic Control*, vol. 64, no. 10, pp. 4321–4328, 2019.
- [28] W. H. Heemels, M. Donkers, and A. R. Teel, “Periodic event-triggered control for linear systems,” *IEEE Transactions on Automatic Control*, vol. 58, no. 4, pp. 847–861, 2012.
- [29] G. Guo, L. Ding, and Q.-L. Han, “A distributed event-triggered transmission strategy for sampled-data consensus of multi-agent systems,” *Automatica*, vol. 50, no. 5, pp. 1489–1496, 2014.
- [30] S. Zheng, P. Shi, R. K. Agarwal, and C. P. Lim, “Periodic event-triggered output regulation for linear multi-agent systems,” *Automatica*, vol. 122, p. 109223, 2020.
- [31] W. Liu and J. Huang, “Leader-following consensus for linear multiagent systems via asynchronous sampled-data control,” *IEEE Transactions on Automatic Control*, vol. 65, no. 7, pp. 3215–3222, 2019.
- [32] W. Yu, W. X. Zheng, G. Chen, W. Ren, and J. Cao, “Second-order consensus in multi-agent dynamical systems with sampled position data,” *Automatica*, vol. 47, no. 7, pp. 1496–1503, 2011.
- [33] N. Huang, Z. Duan, and G. R. Chen, “Some necessary and sufficient conditions for consensus of second-order multi-agent systems with sampled position data,” *Automatica*, vol. 63, pp. 148–155, 2016.
- [34] F. Yan, G. Gu, and X. Chen, “A new approach to cooperative output regulation for heterogeneous multi-agent systems,” *SIAM Journal on Control and Optimization*, vol. 56, no. 3, pp. 2074–2094, 2018.
- [35] C. Godsil and G. F. Royle, *Algebraic graph theory*. Springer Science & Business Media, 2013, vol. 207.
- [36] Y. Yan and J. Huang, “Cooperative output regulation of discrete-time linear time-delay multi-agent systems under switching network,” *Neurocomputing*, vol. 241, pp. 108–114, 2017.
- [37] M. Cao, F. Xiao, and L. Wang, “Event-based second-order consensus control for multi-agent systems via synchronous periodic event detection,” *IEEE Transactions on Automatic Control*, vol. 60, no. 9, pp. 2452–2457, 2015.
- [38] H. Cai, F. L. Lewis, G. Hu, and J. Huang, “The adaptive distributed observer approach to the cooperative output regulation of linear multi-agent systems,” *Automatica*, vol. 75, pp. 299–305, 2017.
- [39] G. D. Khan, Z. Chen, and L. Zhu, “A new approach for event-triggered stabilization and output regulation of nonlinear systems,” *IEEE Transactions on Automatic Control*, vol. 65, no. 8, pp. 3592–3599, 2020.
- [40] W. Ren and E. Atkins, “Distributed multi-vehicle coordinated control via local information exchange,” *International Journal of Robust and Nonlinear Control: IFAC-Affiliated Journal*, vol. 17, no. 10-11, pp. 1002–1033, 2007.